Lawrence Berkeley National Laboratory
LBL Publications

Title

Theory and computation of electromagnetic fields and thermomechanical structure interaction for systems undergoing large deformations

Permalink

https://escholarship.org/uc/item/43h0k7g8

Authors

Abali, BE
Queiruga, AF

Publication Date

2019-10-01

DOI

10.1016/j.jcp.2019.05.045

Peer reviewed

eScholarship.org Powered by the California Digital Library
University of California

arXiv:1803.10551v1 [cs.CE] 28 Mar 2018

Theory and computation of electromagnetic fields and thermomechanical structure interaction for systems undergoing large deformations

B. E. Abali * A. F. Queiruga†

Abstract

The governing equations for electromagneto-thermomechanical systems are well established and thoroughly derived in the literature, but have been limited to small deformations. This assumption provides an "ease" in the formulation: electromagnetic fields are governed in a EULERian frame, whereby the thermomechanics is solved in a LAGRANGEan frame. It is possible to map the EULERian frame to the current placement of the matter and the LAGRANGEan frame to a reference placement. The assumption of small deformations eliminates the distinction between current and initial placement such that electromagnetism and thermomechanics are formulated in the same frame.

We present a rigorous and thermodynamically consistent derivation of governing equations for fully coupled electromagneto-thermomechanical systems properly handling finite deformations. A clear separation of the different frames is necessary. There are various attempts to formulate electromagnetism in the LAGRANGEan frame, or even to compute all fields in the current placement. Both formulations are challenging and heavily discussed in the literature. In this work, we propose another solution scheme that exploits the capabilities of advanced computational tools. Instead of amending the formulation, we can solve thermomechanics in the LAGRANGEan frame and electromagnetism in the EULERian frame and manage the interaction between the fields. The approach is similar to its analog in fluid structure interaction, but additionally challenging because the electromagnetic governing equations must also be solved within the solid body while following their own different set of transformation rules. We further present a mesh-morphing algorithm necessary to accommodate finite deformations to solve the electromagnetic fields outside of the material body. We illustrate the use of the new formulation by developing an open-source implementation using the FEniCS package and applying this implementation to several engineering problems in electromagnetic structure interaction undergoing large deformations.

1. Introduction

The theory of electromagnetism started with [53] and is often explained by MAXWELL's equations. The theory has been continuously developed and amended, notably in the 1950s during the renaissance of thermodynamics. The inclusion of mechanics and thermodynamics into the theory of electromagnetism is governed by balance laws; however, there is no consensus among the scientific community. The lack of consensus owes to various challenges in the formulation and the lack of experimental verifications for proposed formulations. For example, there are different representations of MAXWELL's equations, cf. [67] and [19, Sect. II]. Another challenge occurs due to the different invariance properties of balance laws and MAXWELL's equations, raising questions about the proper forms of electromagnetic interaction equations in matter. The readers are directed to [87, §286] for some of these different formulations.

In addition to agreeing upon the governing equations for electromagneto-thermomechanical fields, we must also define the constitutive responses, i.e., the equations dictating the material behavior. Typically, phenomenological equations are constructed relying on experiments, which limit their applicability to measurement conditions. In order to define generic relations, we want to follow a consistent theoretical derivation through thermodynamics. However, there is no consensus for deriving thermodynamically sound constitutive equations

*Corresponding author. Technische Universität Berlin; email: bilenemek@abali.org
†Lawrence Berkeley National Laboratory; email: afqueiruga@lbl.gov

for electromagnetically polarizable systems. The challenge again lies in the formulation of balance laws, especially on the balance of energy, which has been discussed by [22]. There exist a few complete theories for polarized deformable media, as those of [32, Chap. XIII], [60, Chap. 9], [23, Chap. 5], [43, Chap. 15], [14], and [1, Chap. 3]. Each of the mentioned formulations is different, and an experimental verification to determine the correctness is still missing.

Computational methods help us to simulate and comprehend realistic applications in two ways. First, we can estimate response of a system before manufacturing. Secondly, we can design experiments for validating or even discovering an accurate representation of the physical world. Several computational strategies exist for solving coupled equations by means of finite element simulations. For detailed reviews, see [10], [34], and [90]. Different simplifications of the governing equations are employed in order to enable a numerical analysis. For example, restriction to the quasi-static case can be seen in [94], [3] and [72]. A case without free charges was presented by [84]. A magneto-elasto-static case has been suggested in [82]. In [55] the temperature distribution is added again for the static case. A complete dynamical description and transient computation of electromagneto-thermomechanical has been proposed recently in [73] and [2]. In most of these works, the formulations are established on the same configuration. If the electromagnetic fields interact with solid bodies, a LAGRANGEan frame is chosen, where each coordinate maps to a material particle. In the case of fluids, a EULERian frame is chosen, wherein each coordinate indicates a fixed position in ordinary (physical) space. Solving electromagnetic fields in a EULERian frame and thermomechanical fields in a LAGRANGEan frame is not a new idea. Among others, [40], [75], [83], [7], [91], and [71] have developed computational strategies to overcome different problems. In all aforementioned works, governing equations differ due to the different simplifications and assumptions used. Instead of a comparison of different works, we start from the beginning with a new derivation of the equations based on the continuum mechanics such that any assumptions and weaknesses in the methodology can be precisely identified and addressed.

We begin by outlining the theory in Section 2, following [1, Chap. 3] most closely. The main objective is to compute the *primitive* variables for solids under finite deformation, namely the temperature T and displacement $\boldsymbol{u}$, and to compute for the entirety of space encompassed by the computational domain the so-called electromagnetic potentials ϕ, $\boldsymbol{A}$. In the formulation we will use different frames, where $\boldsymbol{X}$ denotes the reference position of a massive particle, and $\boldsymbol{x}$ indicates a position in the ordinary space. The close the theory by developing comprehensive thermodynamically consistent constitutive equations for solids in Section 3. We discuss the issues with solving these equations using the finite element method in Section 4. To address the large deformations of the solid mesh embedded in the mesh of the electromagnetic computational domain, we present a mesh morphing algorithm that enables the calculations by keeping a valid mesh in the space surrounding the body. The variational forms and new algorithms are implemented with aid of the novel collection of open-source packages provided by the FEniCS project [36, 48]. The library containing the presented mesh morphing algorithm and other helper routines is released at `https://github.com/afqueiruga/afqsfenicsutil` under the GNU Lesser General Public License [28]. In Section 5, we present three example simulations of example applications to electromagnetic devices whose implementations are published at `https://github.com/afqueiruga/EMSI-2018` under the GNU General Public License. We conclude the discussion in Section 6.

2. Governing equations

Consider a solid body $\mathcal{b}$ immersed in air. We will solve electromagnetic fields in the whole domain Ω including a body $\mathcal{b}$ and air, $\Omega_{\text{air}} = \Omega \backslash \mathcal{b}$. The solid body undergoes a deformation. The mechanical fields will be computed within the body $\mathcal{b}$. Although the surrounding air might be set in motion due to the deformation of the solid body and its own electromagnetic interactions, we will ignore the fluid motion. For certain applications, we might want to solve the temperature distribution within the air as well, but it is not of interest for now. We choose to compute the temperature distribution only within the solid body to save computational time. Therefore, we aim at determining governing equations for electromagnetic fields within Ω and for thermomechanical fields within $\mathcal{b}$. At the interface $I = \Omega \cap \partial\mathcal{b}$, we need to discuss the interaction and satisfy another set of governing equations. We motivate the theory in three subsections:

- specifying the governing equations for electromagnetic fields in the whole domain;
- specifying the governing equations for for thermomechanical fields in the solid body;
- specifying the jump conditions on the interface between the solid body and its surroundings.

We will use Cartesian coordinates and the usual tensor index notation with the EINSTEIN summation convention over repeated indices.

2.1. Electromagnetic fields

The main objective in electromagnetism is to obtain the electric field, $\boldsymbol{E}$, and the magnetic flux density, $\boldsymbol{B}$ (an area density). SI units are the most appropriate choice for thermomechanical couplings, where the electric field is measured in V(olt)/m(eter) and the magnetic flux density is measured in T(esla). We start off with FARADAY's law:

$$\Big(\int_S \mathcal{B}_i \,\mathrm{d}a_i\Big)^{\bullet} = -\int_{\partial \mathcal{S}} \mathcal{E}_i \,\mathrm{d}\ell_i \ , \tag{1}$$

defined on arbitrarily moving surface S with the electric field measured on the co-moving frame, $\boldsymbol{\mathcal{E}}$, as well as the magnetic flux on the co-moving frame, $\boldsymbol{\mathcal{B}}$. In other words, the measurement device is installed on S and moves with it. Assume that the domain S defined in $\boldsymbol{x}$ moves with the velocity $\boldsymbol{x}^{\bullet} = \boldsymbol{w}$ measured with respect to the laboratory frame that is set to be fixed (not moving). In order to define a velocity as a measurable quantity, we have to declare one frame without possessing a velocity. Of course a laboratory frame on Earth moves with respect to other planets and stars; however, we declare and maintain the laboratory frame as being fixed such that every motion detected in that frame acquires a velocity. Since $\boldsymbol{\mathcal{B}}$ and $\boldsymbol{\mathcal{E}}$ are detected on a moving frame, we need their transformations to the laboratory frame,

$$\mathcal{E}_i = E_i + (\boldsymbol{w} \times \boldsymbol{B})_i \ , \quad \mathcal{B}_i = B_i \ , \tag{2}$$

for the non-relativistic case, where the magnitude of the domain velocity is small with respect to the speed of light in vacuum, $|\boldsymbol{w}| \ll c$. By using STOKES's theorem as well as the identity

$$(\,\mathrm{d}a_i)^{\bullet} = \Big(\frac{\partial w_k}{\partial x_k}\delta_{ji} - \frac{\partial w_j}{\partial x_i}\Big)\,\mathrm{d}a_j \ , \tag{3}$$

we acquire the local form of FARADAY's law:

$$\begin{gathered}
B_j^{\bullet} + B_i\Big(\frac{\partial w_k}{\partial x_k}\delta_{ji} - \frac{\partial w_j}{\partial x_i}\Big) = -\operatorname{curl}(\boldsymbol{E} + \boldsymbol{w} \times \boldsymbol{B})_j \ , \\
\frac{\partial B_j}{\partial t} + \frac{\partial B_j}{\partial x_k}w_k + B_j\frac{\partial w_k}{\partial x_k} - B_i\frac{\partial w_j}{\partial x_i} + \epsilon_{jkl}\frac{\partial E_l}{\partial x_k} + \epsilon_{jkl}\epsilon_{lmn}\frac{\partial w_m B_n}{\partial x_k} = 0 \ , \\
\frac{\partial B_j}{\partial t} + \frac{\partial B_j w_k}{\partial x_k} - B_i\frac{\partial w_j}{\partial x_i} + \epsilon_{jkl}\frac{\partial E_l}{\partial x_k} + \frac{\partial w_j B_k}{\partial x_k} - \frac{\partial w_k B_j}{\partial x_k} = 0 \ , \\
\frac{\partial B_j}{\partial t} + \epsilon_{jkl}\frac{\partial E_l}{\partial x_k} + w_j\frac{\partial B_k}{\partial x_k} = 0 \ ,
\end{gathered} \tag{4}$$

using the identity $\epsilon_{jkl}\epsilon_{lmn} = \delta_{jm}\delta_{kn} - \delta_{jn}\delta_{km}$. Moreover, we can consider the special case where the surface S is a closed hull, for example boundary of a continuum body, $\partial\mathcal{b}$, without a line boundary such that the right-hand side in Eq. (1) vanishes and we obtain after an integration in time

$$\int_{\partial\mathcal{b}} B_i \,\mathrm{d}a_i = \text{const.}|_t \ . \tag{5}$$

If we select the initial magnetic flux as zero, the integration constant drops. Since the selected boundary is a closed hull, we can apply GAUSS's law and acquire

$$\frac{\partial B_i}{\partial x_i} = 0 \ . \tag{6}$$

We have obtained the so-called first set of MAXWELL's equations:

$$\frac{\partial B_i}{\partial x_i} = 0 \ , \quad \frac{\partial B_i}{\partial t} + \epsilon_{ijk}\frac{\partial E_k}{\partial x_j} = 0 \ . \tag{7}$$

These equations are universal, i.e., they hold for any material and even in the case of no massive particles (vacuum). Hence, the coordinate $\boldsymbol{x}$ denotes a location or point in the (ordinary) space. We call it a *spatial* frame since the coordinates indicate a position in space. There might be a massive particle occupying the

location $\boldsymbol{x}$, but the coordinate still indicates a location in space without any relation to that particle or its motion. The sought-after electromagnetic fields, $\boldsymbol{E}$ and $\boldsymbol{B}$, have to satisfy the latter equations. Their solution is obtained by using the following *ansatz* functions:

$$E_i = -\frac{\partial \phi}{\partial x_i} - \frac{\partial A_i}{\partial t} \ , \quad B_i = \epsilon_{ijk} \frac{\partial A_k}{\partial x_j} \ , \tag{8}$$

such that now we search for the electric potential ϕ in V and magnetic potential $\boldsymbol{A}$ in T m for $\forall x_i \in \Omega$. If we can compute the electromagnetic potentials, we readily obtain the electromagnetic fields from the latter equations. Since we aim to describe the system using only four components $\{\phi, A_1, A_2, A_3\}$ instead of six components $\{E_1, E_2, E_3, B_1, B_2, B_3\}$, there are two scalar degrees of freedom that are not uniquely determined; namely $\partial\phi/\partial t$ and $\partial A_i/\partial x_i$ can be chosen freely. This so-called *gauge* freedom is used to eliminate many numerical problems, see [9], we will use Lorenz's gauge:

$$\frac{\partial \phi}{\partial t} = -c^2 \frac{\partial A_i}{\partial x_i} \ , \quad c^2 = \frac{1}{\mu_0 \varepsilon_0} \ , \tag{9}$$

with the speed of light in vacuum, c, and the precisely known universal constants:

$$\varepsilon_0 = 8.85 \cdot 10^{-12} \, \mathrm{A\,s/(V\,m)} \ , \quad \mu_0 = 12.6 \cdot 10^{-7} \, \mathrm{V\,s/(A\,m)} \ . \tag{10}$$

In order to motivate the second set of Maxwell's equations, we use the balance of electric charge in an open domain Ω where the domain moves with $\boldsymbol{w}$

$$\Big(\int_\Omega q \, \mathrm{d}v \Big)^{\boldsymbol{\cdot}} = \int_{\partial\Omega} \Big(q(w_i - v_i) - \jmath_i \Big) \, \mathrm{d}a_i \ . \tag{11}$$

The electric charge density q in C(oulomb)/m^3 is searched for and electric current (area density) $\boldsymbol{\jmath}$ in A(mpere)/m^2 needs to be declared. If a massive particle conveying an electric charge of q enters the domain, the amount of charge within the domain increases. The particle moves with $\boldsymbol{v}$ and can enter the domain only across its boundary $\partial\Omega$, if the relative velocity $\boldsymbol{w} - \boldsymbol{v}$ is positive along the surface direction, $\mathrm{d}a_i = n_i \, \mathrm{d}a$, we refer to [59], [62] for a discussion of balance equations in open and moving domain. The surface direction $\boldsymbol{n}$ points outward the domain. We can again get the local form after using the rate of the volume element in the spatial frame moving with $\boldsymbol{w}$,

$$\mathrm{d}v^{\boldsymbol{\cdot}} = \frac{\partial w_i}{\partial x_i} \, \mathrm{d}v \ , \tag{12}$$

and apply Gauss's law:

$$\begin{aligned} q^{\boldsymbol{\cdot}} + q \frac{\partial w_i}{\partial x_i} &= \frac{\partial}{\partial x_i} \Big(q(w_i - v_i) - \jmath_i \Big) \ , \\ \frac{\partial q}{\partial t} + \frac{\partial q w_i}{\partial x_i} &= \frac{\partial}{\partial x_i} \Big(q(w_i - v_i) - \jmath_i \Big) \ , \\ \frac{\partial q}{\partial t} + \frac{\partial J_i}{\partial x_i} &= 0 \ , \end{aligned} \tag{13}$$

where $J_i = \jmath_i + q v_i$ represents the electric current measured in the laboratory frame. Since the domain Ω has a well-defined boundary, $\partial\Omega$, we can introduce a charge potential $\boldsymbol{\mathcal{D}}$ measured on the moving domain as follows

$$\int_\Omega q \, \mathrm{d}v = \int_{\partial\Omega} \mathcal{D}_i \, \mathrm{d}a_i \ , \tag{14}$$

leading to the following Maxwell equation after applying Gauss's law

$$q = \frac{\partial \mathcal{D}_i}{\partial x_i} \ . \tag{15}$$

The charge potential $\boldsymbol{\mathcal{D}}$ in C/m^2 is quite general stemming from the *total* charge q in space. Now by using the charge potential, we rewrite the balance of charge in an open domain with a closed boundary, $\partial\partial\Omega = \{\}$,

$$\Big(\int_{\partial\Omega} \mathcal{D}_i \, \mathrm{d}a_i \Big)^{\boldsymbol{\cdot}} = \int_{\partial\Omega} \Big(q(w_i - v_i) - \jmath_i \Big) \, \mathrm{d}a_i \ , \tag{16}$$

as a balance equation on a surface with its boundary ∂S

$$\Big(\int_S \mathcal{D}_i \,\mathrm{d}a_i\Big)^{\cdot} = \int_{\partial S} \mathcal{H}_i \,\mathrm{d}\ell_i + \int_S \Big(q(w_i - v_i) - \mathcal{J}_i\Big)\,\mathrm{d}a_i \ , \tag{17}$$

where the flux on the surface boundary $\boldsymbol{\mathcal{H}}$ is called the current potential measured on the moving surface. Transformations of the charge and current potentials from the moving frame to the laboratory (fixed) frame read

$$\mathcal{D}_i = D_i \ , \quad \mathcal{H}_i = H_i + (\boldsymbol{D}\times\boldsymbol{w})_i \ , \tag{18}$$

for the non-relativistic case. Now we can insert the rate of the area element, apply Stokes's theorem, and obtain the local form

$$\begin{gathered}
\dot{D_j} + D_i\Big(\frac{\partial w_k}{\partial x_k}\delta_{ji} - \frac{\partial w_j}{\partial x_i}\Big) = \mathrm{curl}(\boldsymbol{H} + \boldsymbol{D}\times\boldsymbol{w})_j + qw_j - J_j \ , \\
\frac{\partial D_j}{\partial t} + \frac{\partial D_j}{\partial x_i}w_i + D_j\frac{\partial w_k}{\partial x_k} - D_i\frac{\partial w_j}{\partial x_i} = \epsilon_{jkl}\frac{\partial H_l}{\partial x_k} + \epsilon_{jkl}\epsilon_{lmn}\frac{\partial D_m w_n}{\partial x_k} + qw_j - J_j \ , \\
\frac{\partial D_j}{\partial t} + \frac{\partial D_j w_i}{\partial x_i} - D_i\frac{\partial w_j}{\partial x_i} = \epsilon_{jkl}\frac{\partial H_l}{\partial x_k} + \frac{\partial D_j w_k}{\partial x_k} - \frac{\partial D_k w_j}{\partial x_k} + \frac{\partial D_i}{\partial x_i}w_j - J_j \ , \\
\frac{\partial D_j}{\partial t} = \epsilon_{jkl}\frac{\partial H_l}{\partial x_k} - J_j \ .
\end{gathered} \tag{19}$$

We have obtained the second set of Maxwell's equations:

$$q = \frac{\partial D_i}{\partial x_i} \ , \quad \frac{\partial D_j}{\partial t} = \epsilon_{jkl}\frac{\partial H_l}{\partial x_k} - J_j \ , \tag{20}$$

they are universal and hold in the whole domain. The domain can be moving with $\boldsymbol{w}$, the charge and current potentials on the laboratory frame—$\boldsymbol{D}$ and $\boldsymbol{H}$ respectively—do not change at all. Therefore, the domain velocity is arbitrary giving us a freedom to choose the domain velocity freely. We will generate the domain velocity in such a way that the mesh quality remains optimal. This fact will be discussed later.

We have reached the following governing equations:

$$\begin{gathered}
\frac{\partial q}{\partial t} + \frac{\partial J_i}{\partial x_i} = 0 \ , \quad J_i = \mathcal{J}_i + qv_i \ , \quad q = \frac{\partial D_i}{\partial x_i} \ , \\
\frac{\partial D_j}{\partial t} - \epsilon_{jki}\frac{\partial H_i}{\partial x_k} + J_j = 0 \ ,
\end{gathered} \tag{21}$$

in order to compute the electromagnetic potentials, ϕ and $\boldsymbol{A}$. In order to close the equations, the total charge potential and the total current potential need to be expressed in terms of the electromagnetic potentials. The so-called Maxwell–Lorentz aether relations:

$$D_i = \varepsilon_0 E_i \ , \quad H_i = \frac{1}{\mu_0}B_i \ , \tag{22}$$

augmented by Eq. (8) presents the relation closing the coupled governing equations. These equations will be solved in the whole domain, Ω.

2.2. Thermomechanical fields

Consider a continuum body, $\mathcal{b}$, within the domain Ω. This body consists of massive particles with electric charge. Mass (volume) density ρ and specific charge (per mass) z are material dependent variables. Their initial values are known. The total charge z in a material is decomposed as *free* charge $z^{\mathrm{fr.}}$ and *bound* charges $z^{\mathrm{bo.}}$ as follows

$$z = z^{\mathrm{fr.}} + z^{\mathrm{bo.}} \ . \tag{23}$$

Free charges are the valence electrons carrying the electric current effectively in a conductor, they can move large distances. Bound charges are held by the intra-molecular forces and they only move less than the molecular length. Their motion give rise to a decomposition of the charge and current potentials,

$$D_i = \mathfrak{D}_i - P_i \ , \quad H_i = \mathfrak{H}_i + \mathcal{M}_i \ , \tag{24}$$

where the bound charge potential P_i is called an electric polarization and the bound current potential $\mathcal{M}_i$ is called a magnetic polarization. Minus sign is a convention of the declaration of electric polarization in the atomistic scale. Since we already have introduced MAXWELL–LORENTZ aether relation, we need constitutive equations either for $\mathfrak{D}_i$ and $\mathfrak{H}_i$ or for P_i and $\mathcal{M}_i$. By using above definitions we achieve the analogous decomposition for the electric current

$$J_i = J_i^{\text{fr.}} + J_i^{\text{bo.}} \ , \quad J_i^{\text{bo.}} = \frac{\partial P_i}{\partial t} + \epsilon_{ijk} \frac{\partial \mathcal{M}_k}{\partial x_j} \ , \tag{25}$$

see Appendix A for its well-known derivation. The massive particles' initial positions are known and denoted by $\boldsymbol{X}$. Effected by mechanical, thermal, and electromagnetic forces, particles at $\boldsymbol{X}$ displace as much as $\boldsymbol{u}$ and move to $\boldsymbol{x}$ such that $\boldsymbol{u} = \boldsymbol{x} - \boldsymbol{X}$ in m. Moreover, the temperature T in K(elvin) and electromagnetic potentials of particles are necessary to compute. Since we know the initial positions of the (non-congruent) particles, we can use $\boldsymbol{X}$ in order to identify the material particles. We call it a *material* frame since the coordinates indicate material particles' positions. In the material frame, we search for $\boldsymbol{u}$, T, ϕ, and $\boldsymbol{A}$ as functions in space $\boldsymbol{X}$ and time t. Here the space is in a LAGRANGEan frame such that a coordinate value $\boldsymbol{X}$ indicates the same particle throughout the simulation. Initial conditions fail to depend on time, $\partial X_i / \partial t = 0$. We start off with the general balance equation in a volume (with regular points)

$$\left(\int_{\mathfrak{b}} \psi \, \mathrm{d}v \right)^{\cdot} = \int_{\partial \mathfrak{b}} \Phi_j \, \mathrm{d}a_j + \int_{\mathfrak{b}} \rho k \, \mathrm{d}v + \int_{\mathfrak{b}} p \, \mathrm{d}v \ , \tag{26}$$

where rate of the volume density ψ is balanced by the fluxes across the boundary Φ_j, volumetric supply terms k, and production terms p. This balance equation is in the current placement, where $\boldsymbol{x}$ denote the current positions of material particles. We start the simulation with particles at $\boldsymbol{X}$ and they move to $\boldsymbol{x}$. The current positions of particles change in time such that $\dot{x_i} = v_i$ in the material frame. Therefore, the rate of a volume element in the material frame reads

$$\mathrm{d}v^{\cdot} = \frac{\partial v_i}{\partial x_i} \, \mathrm{d}v \ , \tag{27}$$

leading to the following local form after applying GAUSS's law

$$\frac{\partial \psi}{\partial t} + \frac{\partial}{\partial x_j} (v_j \psi - \Phi_j) - k = p \ . \tag{28}$$

In the local form we write the production term on the right-hand side in order to emphasize the conserved quantities. If the production term vanishes, the variable in the balance equation is a conserved quantity. We axiomatically start with the balance equations for the mass, total momentum, and total energy as given in Table 1. It is important to emphasize that we assume that the mass, total momentum, and total energy are all

Table 1: Volume densities in the balance equations and their supply terms, flux terms, and production terms.

ψ	Φ_j	k	p
ρ	0	0	0
$\rho v_i + \mathcal{G}_i$	$\sigma_{ji} + m_{ji}$	ρf_i	0
$\rho e^{\text{m.}} + e^{\text{f.}}$	$\zeta_i + \mathcal{P}_i$	ρs	0

conserved quantities. Now, the balance equations read

$$\begin{aligned} \frac{\partial \rho}{\partial t} + \frac{\partial v_j \rho}{\partial x_j} &= 0 \ , \\ \frac{\partial}{\partial t} (\rho v_i + \mathcal{G}_i) + \frac{\partial}{\partial x_j} \big(v_j \rho v_i - \sigma_{ji} - m_{ji} \big) - \rho f_i &= 0 \ , \\ \frac{\partial}{\partial t} (\rho e^{\text{m.}} + e^{\text{f.}}) + \frac{\partial}{\partial x_j} \big(v_j \rho e^{\text{m.}} - \zeta_j - \mathcal{P}_j \big) - \rho s &= 0 \end{aligned} \tag{29}$$

Mass density, ρ, has a convective flux, $\boldsymbol{v}\rho$, because mass is conveyed by the moving material particles. Total momentum density, $\rho \boldsymbol{v} + \boldsymbol{\mathcal{G}}$, consists of a part due to matter, $\rho \boldsymbol{v}$, and another part due to the electromagnetic field, $\boldsymbol{\mathcal{G}}$. Matter and the electromagnetic field are coupled; however, we will be decomposing terms by splitting the fields along their interaction. Consider a massive object moving in an electromagnetic field in a way that the

electromagnetic field does not alter, i.e., matter and field are independent. Of course, as given in the balance of momentum, the existing field's rate applies forces on the moving charges and a massive object has usually (bound) electric charges such that its acceleration leads to a change in the velocity, in other words, matter and field are coupled. Thus, it is intuitive to treat the electromagnetic field and matter separately (independently) in a coupled manner. We can always fix matter and vary the field, and *vice versa*.

In the balance of momentum, convective flux is only on the part due to the matter. Non-convective flux of momentum, $\boldsymbol{\sigma}+\boldsymbol{m}$, is also decomposed into CAUCHY's stress, $\boldsymbol{\sigma}$, and an electromagnetic stress, $\boldsymbol{m}$. The specific supply term, $\boldsymbol{f}$, is the body force because of gravity. Total energy density, $\rho e^{\mathrm{m.}}+e^{\mathrm{f.}}$, is decomposed into matter and field energies, as well as non-convective fluxes, ζ_i and $\mathcal{P}_i$, respectively. Again only the energy due to matter is conveyed by moving massive particles, $\boldsymbol{v}\rho e^{\mathrm{m.}}$, as a convective flux. The specific supply term, s, is given. All the other terms will be defined in the following discussion.

In the above formulation, the electromagnetic momentum, stress, energy, and flux are the key terms for the correct interaction. Hence it is customary to introduce the following relations:

$$\begin{aligned}\frac{\partial \mathcal{G}_i}{\partial t} &= \frac{\partial m_{ji}}{\partial x_j} - \mathcal{F}_i \ , \\ \frac{\partial e^{\mathrm{f.}}}{\partial t} &= \frac{\partial \mathcal{P}_j}{\partial x_j} - \pi \ ,\end{aligned} \tag{30}$$

where the electromagnetic momentum $\boldsymbol{\mathcal{G}}$ and electromagnetic stress $\boldsymbol{m}$ are related to the electromagnetic force (density), $\boldsymbol{\mathcal{F}}$, analogously, electromagnetic energy (density) $e^{\mathrm{f.}}$ and electromagnetic flux $\boldsymbol{\mathcal{P}}$ are related to an electromagnetic power (density), π. These mathematical identities might be called balance equations; however, we refrain ourselves from using this terminology, since there is an ongoing discussion in the literature about the correctness of this terminology. It is obvious that we can insert the latter identities and renew the table as in Table 2.

Table 2: Volume densities in the balance equations and their supply terms, flux terms, and production terms.

ψ	Φ_j	k	p
ρ	0	0	0
ρv_i	σ_{ji}	ρf_i	$\mathcal{F}_i$
$\rho e^{\mathrm{m.}}$	ζ_i	ρs	π

Now the momentum and energy balances read

$$\begin{aligned}\frac{\partial \rho v_i}{\partial t} + \frac{\partial}{\partial x_j}\big(v_j \rho v_i - \sigma_{ji}\big) - \rho f_i = \mathcal{F}_i \ , \\ \frac{\partial \rho e^{\mathrm{m.}}}{\partial t} + \frac{\partial}{\partial x_j}\big(v_j \rho e^{\mathrm{m.}} - \zeta_j\big) - \rho s = \pi \ .\end{aligned} \tag{31}$$

After using the balance of mass and the material derivative

$$\frac{\mathrm{d}}{\mathrm{d}t} = \frac{\partial}{\partial t} + v_i \frac{\partial}{\partial x_i} \ , \tag{32}$$

they are

$$\begin{aligned}\rho \frac{\mathrm{d}v_i}{\mathrm{d}t} - \frac{\partial \sigma_{ji}}{\partial x_j} - \rho f_i = \mathcal{F}_i \ , \\ \rho \frac{\mathrm{d}e^{\mathrm{m.}}}{\mathrm{d}t} - \frac{\partial \zeta_i}{\partial x_i} - \rho s = \pi \ ,\end{aligned} \tag{33}$$

furnishing the consequence that momentum and energy of matter are not conserved quantities in the case of electromagnetism. The production terms $\boldsymbol{\mathcal{F}}$ and π need to be defined in such a way that they vanish if electromagnetic fields are zero. Unfortunately, their definitions are challenging and there exists no consensus between the scientific community, see for example [64, 52, 29, 11]. We will propose terms in accordance with

Eq. (30), which is the method of derivation used in [49, Eq. (15)], [38, Chap. 1], [32, Chap. XIV], [30, Chap. 8], [51, Sect. 3.3]. If the electromagnetic momentum, $\mathcal{G}_i$, is defined, then, as a consequence of Eq. $(30)_1$, we can deduce the electromagnetic stress, m_{ji}, and the electromagnetic force density, $\mathcal{F}_i$. By following [8] we emphasize that different choices are perfectly appropriate. The reasoning can be explained by: the manifestation of a force as a contact force leads a term into the electromagnetic stress, whereas as a body force leads to a term causing a momentum rate. In the atomistic scale we know that all electromagnetic forces are contact forces. However, in the macroscopic scale we can observe a momentum change due to the electromagnetic fields such that declaring a body force is also suitable. Any choice of $\boldsymbol{\mathcal{G}}$, $\boldsymbol{m}$, and $\boldsymbol{\mathcal{F}}$ is possible as long as the relations in Eq. (30) are fulfilled. Analogously, we can choose an electromagnetic flux, $\boldsymbol{\mathcal{P}}$, leading to the field energy and power. The choices cannot be justified or falsified by experiments, since we cannot detect contact forces and motion independently. Every sensor—used for detecting contact forces—depends on material properties coupling motion with electromagnetism.

Now we introduce a specific (per mass) internal energy, u, by decomposing the energy of matter in kinetic and internal energy

$$e^{\text{m.}} = \frac{1}{2} v_i v_i + u \ . \tag{34}$$

By inserting the latter into the balance of energy and using the balance of momentum,

$$\begin{aligned} \rho \frac{\mathrm{d}v_i}{\mathrm{d}t} v_i + \rho \frac{\mathrm{d}u}{\mathrm{d}t} - \frac{\partial \zeta_j}{\partial x_j} - \rho s = \pi \ , \\ \Big(\frac{\partial \sigma_{ji}}{\partial x_j} + \rho f_i + \mathcal{F}_i \Big) v_i + \rho \frac{\mathrm{d}u}{\mathrm{d}t} - \frac{\partial \zeta_j}{\partial x_j} - \rho s = \pi \ , \\ \rho \frac{\mathrm{d}u}{\mathrm{d}t} - \frac{\partial}{\partial x_j} \big(\zeta_j - \sigma_{ji} v_i \big) - \rho (s - f_i v_i) = \sigma_{ji} \frac{\partial v_i}{\partial x_j} + \pi - \mathcal{F}_i v_i \ , \end{aligned} \tag{35}$$

we have obtained the balance of internal energy. Obviously, we need to define π and $\mathcal{F}_i$ before we proceed. Among many different possibilities, the following choice leads to a thermodynamically consistent formulation. Suppose that we simply choose the electromagnetic momentum as follows

$$\mathcal{G}_i = (\mathfrak{D} \times \boldsymbol{B})_i \ , \tag{36}$$

which is called Minkowski's momentum. It leads to the following electromagnetic stress and force

$$\begin{aligned} m_{ji} &= -\frac{1}{2} \delta_{ji} (H_k B_k + D_k E_k) + H_i B_j + D_j E_i \ , \\ \mathcal{F}_i &= \rho z E_i + \epsilon_{ijk} J_j B_k - \epsilon_{ijk} \frac{\partial P_j}{\partial t} B_k - \epsilon_{ijk} P_j \frac{\partial B_k}{\partial t} \ , \end{aligned} \tag{37}$$

after using Maxwell's equations, see Appendix B for its derivation. Suppose now that we choose the electromagnetic flux as Poynting's vector

$$\mathcal{P}_i = \epsilon_{ijk} \mathfrak{H}_j E_k = \big(\mathfrak{H} \times \boldsymbol{E} \big)_i \ , \tag{38}$$

in this case, as shown in Appendix C, we obtain

$$e^{\text{f.}} = P_i E_i - B_i \mathcal{M}_i + \frac{1}{2} \big(D_i E_i + H_i B_i \big) \ , \quad \pi = J_i^{\text{fr.}} E_i - P_i \frac{\partial E_i}{\partial t} + B_i \frac{\partial \mathcal{M}_i}{\partial t} \ , \tag{39}$$

The production term due to the field can be rewritten by using the above definition of the electromagnetic force

$$\begin{aligned} \mathcal{F}_i v_i = \frac{\partial}{\partial x_j} \Big((-P_j E_i + \mathcal{M}_i B_j) v_i + \big(\mathfrak{H} \times \boldsymbol{E} \big)_j \Big) + \frac{\partial}{\partial t} \Big(B_i \mathcal{M}_i - P_j E_j - \frac{1}{2} D_j E_j - \frac{1}{2} B_i H_i \Big) - \\ - (-P_j E_i + \mathcal{M}_i B_j) \frac{\partial v_i}{\partial x_j} - \mathcal{E}_i \mathcal{J}_i^{\text{fr.}} + P_i \frac{\mathrm{d}E_i}{\mathrm{d}t} - B_i \frac{\mathrm{d}\mathcal{M}_i}{\mathrm{d}t} = \frac{\partial}{\partial x_j} \Big((-P_j E_i + \mathcal{M}_i B_j) v_i \Big) + \\ \underbrace{+ \frac{\partial \mathcal{P}_j}{\partial x_j} - \frac{\partial e^{\text{f.}}}{\partial t}}_{\pi} - (-P_j E_i + \mathcal{M}_i B_j) \frac{\partial v_i}{\partial x_j} - \mathcal{E}_i \mathcal{J}_i^{\text{fr.}} + P_i \frac{\mathrm{d}E_i}{\mathrm{d}t} - B_i \frac{\mathrm{d}\mathcal{M}_i}{\mathrm{d}t} . \end{aligned} \tag{40}$$

We refer to [1, Sect. 3.5] for its derivation based only on subsequent use of Maxwell's equations and Maxwell–

Lorentz aether relations. Now the balance of internal energy reads

$$\begin{aligned}\rho\frac{\mathrm{d}u}{\mathrm{d}t} - \frac{\partial}{\partial x_j}\Big(\zeta_j - (\sigma_{ji} - P_jE_i + \mathcal{M}_iB_j)v_i\Big) - \rho(s - f_iv_i) = \\ = \big(\sigma_{ji} - P_jE_i + \mathcal{M}_iB_j\big)\frac{\partial v_i}{\partial x_j} + \mathcal{E}_i\jmath_i^{\mathrm{fr.}} - P_i\frac{\mathrm{d}E_i}{\mathrm{d}t} + B_i\frac{\mathrm{d}\mathcal{M}_i}{\mathrm{d}t}\ .\end{aligned} \tag{41}$$

We emphasize that this derivation holds for every material, we have only used one assumption for choosing the electromagnetic momentum. Conventionally, the non-convective flux term of the internal energy is called the heat flux:

$$-q_j = \zeta_j - (\sigma_{ji} - P_jE_i + \mathcal{M}_iB_j)v_i\ , \tag{42}$$

with the minus sign appearing because heat pumped into the system (against the surface normal) is declared as a positive work. The supply of the internal energy is a given term and is called the radiant heat:

$$r = s - f_iv_i\ . \tag{43}$$

The production term

$$\Gamma = (\sigma_{ji} - P_jE_i + \mathcal{M}_iB_j)\frac{\partial v_i}{\partial x_j} + \mathcal{E}_i\jmath_i^{\mathrm{fr.}} - P_i\frac{\mathrm{d}E_i}{\mathrm{d}t} + B_i\frac{\mathrm{d}\mathcal{M}_i}{\mathrm{d}t}\ , \tag{44}$$

will be especially useful in the following section for deriving the constitutive equations.

Now by using mass balance and Gauss's law, we can obtain the global forms of mass, total momentum, and internal energy balance equations in the current placement:

$$\begin{gathered}\left(\int_{\mathfrak{b}}\rho\,\mathrm{d}v\right)^{\cdot} = 0\ , \quad \left(\int_{\mathfrak{b}}\rho v_i\,\mathrm{d}v\right)^{\cdot} = \int_{\partial\mathfrak{b}}\sigma_{ji}\,\mathrm{d}a_j + \int_{\mathfrak{b}}\rho f_i\,\mathrm{d}v + \int_{\mathfrak{b}}\mathcal{F}_i\,\mathrm{d}v\ , \\ \left(\int_{\mathfrak{b}}\rho u\,\mathrm{d}v\right)^{\cdot} = -\int_{\partial\mathfrak{b}}q_i\,\mathrm{d}a_i + \int_{\mathfrak{b}}\rho r\,\mathrm{d}v + \int_{\mathfrak{b}}\Gamma\,\mathrm{d}v\end{gathered} \tag{45}$$

These balance equations are in the current placement given in $\boldsymbol{x}$, but we search for thermomechanical fields as functions in space $\boldsymbol{X}$ with the reference placement, in which the mass density, displacement, and temperature are known. As the initial conditions are known, for reference placement we choose the initial placement. The volume and area elements are transformed to the initial placement by

$$\mathrm{d}v = J\,\mathrm{d}V\ , \quad \mathrm{d}a_j = \mathrm{d}A_kJ(\boldsymbol{F}^{-1})_{kj}\ , \tag{46}$$

with the deformation gradient and its determinant defined by

$$F_{ij} = \frac{\partial x_i}{\partial X_j} = \frac{\partial u_i}{\partial X_j} + \delta_{ij}\ , \quad J = \det(\boldsymbol{F})\ . \tag{47}$$

Since the volume element in the initial placement is constant in time, after inserting the transformation and using Gauss's law, we obtain the balance equations in a Lagrangean frame

$$\begin{aligned}\rho J = \text{const.}\big|_t = \rho_0\ , \\ \rho_0\frac{\partial v_i}{\partial t} = \frac{\partial}{\partial X_k}\Big(J(\boldsymbol{F}^{-1})_{kj}\sigma_{ji}\Big) + \rho_0f_i + J\mathcal{F}_i\ , \\ \rho_0\frac{\partial u}{\partial t} = -\frac{\partial}{\partial X_k}\Big(J(\boldsymbol{F}^{-1})_{kj}q_j\Big) + \rho_0r + J\,\Gamma\ ,\end{aligned} \tag{48}$$

where each coordinate in space $\boldsymbol{X}$ denotes a material particle. We need constitutive equations in order to close these equations such that we can solve the displacement and temperature by fulfilling them.

2.3. On the interface

Formulation of partial differential equations generally makes the implicit assumption that all fields must be described as continuous in space and all conserved quantities are volume densities. However, this restriction is artificial, as it is perfectly valid to discuss an infinitely thin membrane with mass area density and velocity defined upon it, for example. Electromagnetism in particular has situations where this applies, where surface

charges and currents are prevalent due to material discontinuities, requiring us to develop descriptions for interfaces in addition to the partial differential equations that can only be applied to "smooth" space. Especially between different materials, we obtain "jump" conditions to be satisfied in order to obtain the correct solution.

We name the boundary of the solid body as the interface in order to avoid a confusion to the domain boundary. The interface evolves due to the deformation. Thermomechanical fields are assumed to be computed such that the current placement of the interface is known. We will develop the equations for a generic singular surface and then restrict to the case that the singular surface is the interface. Regions are 3D objects and surfaces are 2D objects embedded in 3D space.

Consider a surface S between two different regions Ω^+ and Ω^- such that $S = \Omega^+ \cap \Omega^-$. On the plus side of the surface—toward which the normal $\boldsymbol{n}$ points—is the region Ω^+ and on the minus side lies Ω^-. We use $\Omega^\pm = \Omega^+ \cup \Omega^- \setminus S = \Omega \setminus S$ to denote the whole domain without the surface. Moreover, the surface is within the domain and its boundary is on the domain's boundary $\partial S = \partial\Omega \cap S$ such that the whole boundary reads $\partial\Omega = \partial\Omega^\pm \cup \partial S$ with $\partial\Omega = (\partial\Omega^+ \setminus S) \cup (\partial\Omega^- \setminus S)$. Note that the boundary of the surface, ∂S, is a 1D loop embedded in 3D space. The surface and domain may be moving with a velocity $\boldsymbol{w}$ and we search for a balance equation in the open domain, i.e., we use a Eulerian frame. Now the general balance equation reads

$$\begin{aligned}\Big(\int_{\Omega^\pm} \psi^V \,\mathrm{d}v + \int_S \psi^S \,\mathrm{d}a\Big)^\cdot = \int_{\partial\Omega^\pm} \Big((w_j - v_j)\psi^V + \Phi_j^V\Big)\,\mathrm{d}a_j + \int_{\partial S} \Big(\psi^S(w_j - v_j) + \Phi_j^S\Big)\,\mathrm{d}\ell_j + \\ + \int_{\Omega^\pm} \big(\rho^V k^V + p^V\big)\,\mathrm{d}v + \int_S \big(\rho^S k^S + p^S\big)\,\mathrm{d}a\ ,\end{aligned} \tag{49}$$

where all volume-related quantities are denoted with a superscript V and surface-related quantities with a superscript S. We are only interested in a special case where the surface is an interface. In other words, the surface itself is a fictitious separation without any mass area-density, $\rho^S = 0$. This restriction allows the following simplification after using the geometric transformations

$$\mathrm{d}v = J\,\mathrm{d}V\ , \quad \mathrm{d}a_j = \mathrm{d}A_k J(\boldsymbol{F}^{-1})_{kj}\ , \quad \mathrm{d}\ell_j = F_{jk}\,\mathrm{d}L_k\ , \quad \mathrm{d}a = \sqrt{\frac{g}{G}}\,\mathrm{d}A\ , \tag{50}$$

where g and G are the determinant of the surface metric tensor in the current and initial frame, respectively. After transforming to the initial placement, we obtain

$$\begin{aligned}\int_{\Omega^\pm} (\psi^V J)^\cdot \,\mathrm{d}V = \int_{\partial\Omega^\pm} \Big((w_j - v_j)\psi^V + \Phi_j^V\Big) J(\boldsymbol{F}^{-1})_{kj}\,\mathrm{d}A_k + \int_{\partial S} \Phi_j^S F_{jk}\,\mathrm{d}L_k + \\ + \int_{\Omega^\pm} \big(\rho^V k^V + p^V\big) J\,\mathrm{d}V + \int_S p^S \sqrt{\frac{g}{G}}\,\mathrm{d}A\ .\end{aligned} \tag{51}$$

For an arbitrary field f, Gauss's law in the initial placement reads

$$\begin{aligned}\int_{\Omega^\pm} \frac{\partial f}{\partial X_k}\,\mathrm{d}V = \int_{\Omega^+} \frac{\partial f}{\partial X_k}\,\mathrm{d}V + \int_{\Omega^-} \frac{\partial f}{\partial X_k}\,\mathrm{d}V = \int_{\partial\Omega^+} f\,\mathrm{d}A_k + \int_{\partial\Omega^-} f\,\mathrm{d}A_k = \\ = \int_{\partial\Omega^+\setminus S} f N_k\,\mathrm{d}A + \int_S f^+ N_k^+\,\mathrm{d}A + \int_{\partial\Omega^-\setminus S} f N_k\,\mathrm{d}A + \int_S f^- N_k^-\,\mathrm{d}A = \int_{\partial\Omega^\pm} f N_k\,\mathrm{d}A + \int_S [\![f N_k]\!]\,\mathrm{d}A\ ,\end{aligned} \tag{52}$$

with f^+ or f^- as the limit value from the region Ω^+ or Ω^- on the interface and N^+ or N^- showing outward the region Ω^+ or Ω^-, respectively. Moreover, we use $[\![f N_k]\!] = f^+ N_k^+ + f^- N_k^-$. We assume that ∂S is closed (no singularities) such that we can use Stokes's law with an arbitrary term f_k as follows

$$\int_{\partial S} f_k\,\mathrm{d}L_k = \int_S \mathrm{curl}(\boldsymbol{f})_k\,\mathrm{d}A_k = \int_S \epsilon_{kji} \frac{\partial f_i}{\partial X_j}\,\mathrm{d}A_k\ . \tag{53}$$

The general balance equation now reads

$$\begin{aligned}\int_{\Omega^\pm} \Big((\psi^V J)^\cdot - \frac{\partial}{\partial X_k}\Big(\big((w_j - v_j)\psi^V + \Phi_j^V\big) J(\boldsymbol{F}^{-1})_{kj}\Big) - \big(\rho^V k^V + p^V\big) J\Big)\,\mathrm{d}V = \\ = \int_S \Big(- \Big[\!\Big[\Big((w_j - v_j)\psi^V + \Phi_j^V\Big) J(\boldsymbol{F}^{-1})_{kj} N_k \Big]\!\Big] + \epsilon_{kli} \frac{\partial \Phi_j^S F_{ji}}{\partial X_l} N_k + p^S \sqrt{\frac{g}{G}}\Big)\,\mathrm{d}A\ .\end{aligned} \tag{54}$$

Since we satisfy the left-hand side within the continuum body, we only need to assure to satisfy the right-hand side on the interface leading to the additional equation on the interface

$$\left[\!\left[\Big((w_j - v_j)\psi^V + \Phi_j^V\Big) J(\boldsymbol{F}^{-1})_{kj} N_k\right]\!\right] = \epsilon_{kli} \frac{\partial \Phi_j^S F_{ji}}{\partial X_l} N_k + p^S \sqrt{\frac{g}{G}} \ . \tag{55}$$

The volume density ψ^V is mass, momentum, internal energy density, as in Table 2; its corresponding flux Φ_j^V is an area density. Analogously, the flux term Φ_j^S is a line density and p^S is a production term; both of them exist only on the interface. For the mass, we know that neither flux nor production terms exist. Therefore, we assume that interface flux and production vanish such as

$$\left[\!\left[(w_j - v_j)\rho J(\boldsymbol{F}^{-1})_{kj} N_k\right]\!\right] = 0 \ , \tag{56}$$

has to be fulfilled. By setting $w_i = v_i$ on the interface, we will satisfy the latter condition—in the implementation, this condition corresponds to forcing the computational mesh to follow the interface. There is, however, a flux term for the momentum. In mechanics the surface tension is the stress on the interface, see [17], [89], [54], [80]. In the case of electromagnetism, the production term on the interface needs to be calculated. As the volumetric production term is given in Eq. $(37)_2$, the area production term is due to the surface charges and currents. Surface charges and currents become important in mixtures with adhesion between particles. For a solid body, we simply neglect these effects and obtain the balance of momentum,

$$\left[\!\left[\Big((w_j - v_j)\rho v_i + \sigma_{ji}\Big) J(\boldsymbol{F}^{-1})_{kj} N_k\right]\!\right] = 0 \ . \tag{57}$$

Since $\boldsymbol{w} = \boldsymbol{v}$ on the interface, the first term drops out leaving

$$\left[\!\left[\sigma_{ji} J(\boldsymbol{F}^{-1})_{kj} N_k\right]\!\right] = 0 \ . \tag{58}$$

Analogously, for the balance of internal energy on the interface, we use $\boldsymbol{v} = \boldsymbol{w}$ and neglect the production as well as the line density flux term (surface heat) such that we obtain

$$[\![q_j N_k J(\boldsymbol{F}^{-1})_{kj}]\!] = 0 \ . \tag{59}$$

We may discuss the displacement field as a continuous variable, meaning that the continuum body fail to have any cracks. An analogous argument holds that all primitive variables are continuous and will be modeled as such. Moreover, the singular surface is an interface in which the surface normal in the current placement has to be continuous. These assertions of continuity yield the following jump conditions:

$$[\![A_i]\!] = 0 \ , \quad [\![\phi]\!] = 0 \ , \quad [\![u_i]\!] = 0 \ , \quad [\![T]\!] = 0 \ , \quad [\![n_j]\!] = [\![N_k J(\boldsymbol{F}^{-1})_{kj}]\!] = 0 \ . \tag{60}$$

In the numerical implementation we need to guarantee that the latter equations apply on the interface. This condition is equivalent imposing that all primitive variables, $\boldsymbol{A}$, ϕ, $\boldsymbol{u}$, T, are continuous within the whole computational domain. As a consequence we have

$$[\![E_i]\!] = 0 \ , \quad [\![D_i]\!] = 0 \ , \quad [\![B_i]\!] = 0 \ , \quad [\![H_i]\!] = 0 \ . \tag{61}$$

Moreover, by deriving Maxwell's equations from the balance equations, the following equations are obtained

$$[\![n_i \mathfrak{D}_i]\!] = 0 \ , \quad [\![\epsilon_{ijk} n_j \mathfrak{H}_k]\!] = 0 \ , \tag{62}$$

under the assumption that no surface charges and currents exist. The jump terms emerge due to the difference of material parameters between the adjacent materials. Therefore, by using the latter, we can also deduce

$$[\![n_i P_i]\!] = 0 \ , \quad [\![\epsilon_{ijk} n_j \mathcal{M}_k]\!] = 0 \ . \tag{63}$$

3. Constitutive equations

Various thermodynamical procedures exist in the literature. They all aim at deriving the constitutive equations for $\boldsymbol{\jmath}^{\text{fr.}}$, $\boldsymbol{\sigma}$, $\boldsymbol{q}$, $\boldsymbol{P}$, and $\boldsymbol{\mathcal{M}}$. We use a similar strategy as in [32] in which the main assumption is that the internal energy is recoverable, leading to an entropy with primary variables but not fluxes. For an extension of the

presented method, see [39].

We will compute the primitive variables in the whole domain: the temperature T, displacement $\boldsymbol{u}$, electric potential ϕ, and magnetic potential $\boldsymbol{A}$. In the end, every proposed constitutive equation has to depend only on the primitive variables (and their space and time derivatives). Since we have general relations in Eq. (8) between electromagnetic fields, $\boldsymbol{E}$, $\boldsymbol{B}$, and electromagnetic potentials, ϕ, $\boldsymbol{A}$, we can also define dependencies with respect to $\boldsymbol{E}$ and $\boldsymbol{B}$. The constitutive equations are necessary where a material occupies a region, they are also called material equations and are defined in the material frame. We start with Eq. $(48)_3$, i.e., the balance of internal energy in the material frame

$$\begin{aligned} \rho_0 \frac{\partial u}{\partial t} &= -\frac{\partial Q_i}{\partial X_i} + \rho_0 r + J\Gamma \ , \quad Q_i = J(\boldsymbol{F}^{-1})_{ij} q_j \ , \\ \Gamma &= \Xi_{ji} \frac{\partial v_i}{\partial x_j} + \mathcal{E}_i \mathcal{J}_i^{\mathrm{fr.}} - P_i \frac{\mathrm{d}E_i}{\mathrm{d}t} + B_i \frac{\mathrm{d}\mathcal{M}_i}{\mathrm{d}t} \ , \quad \Xi_{ji} = \sigma_{ji} - P_j E_i + \mathcal{M}_i B_j \ . \end{aligned} \tag{64}$$

The third and fourth terms in the production of internal energy, Γ, are crucial for deriving the constitutive equations for $\boldsymbol{P}$ and $\boldsymbol{\mathcal{M}}$. The second term in the production of internal energy is called Joule's heat. We will see this term as a purely dissipative phenomenon. The first term can be rewritten

$$J\Xi_{ji} \frac{\partial v_i}{\partial x_j} = J\Xi_{ji} \frac{\partial v_i}{\partial X_k} (\boldsymbol{F}^{-1})_{kj} = N_{ki} \frac{\partial v_i}{\partial X_k} \ , \tag{65}$$

with the nominal stress $N_{ji} = J(\boldsymbol{F}^{-1})_{jk}\Xi_{ki}$ defined in the initial placement. Moreover, we observe in the material frame,

$$\frac{\mathrm{d}F_{ij}}{\mathrm{d}t} = \frac{\mathrm{d}}{\mathrm{d}t} \frac{\partial x_i}{\partial X_j} = \frac{\partial^2 x_i}{\partial t \partial X_j} = \frac{\partial^2 x_i}{\partial X_j \partial t} = \frac{\partial v_i}{\partial X_j} \ , \tag{66}$$

such that the balance of internal energy becomes

$$\rho_0 \frac{\partial u}{\partial t} = -\frac{\partial Q_i}{\partial X_i} + \rho_0 r + N_{ji} \frac{\mathrm{d}F_{ij}}{\mathrm{d}t} + J\mathcal{E}_i \mathcal{J}_i^{\mathrm{fr.}} - JP_i \frac{\mathrm{d}E_i}{\mathrm{d}t} + JB_i \frac{\mathrm{d}\mathcal{M}_i}{\mathrm{d}t} \ . \tag{67}$$

Now we make several assumptions in order to deduce an equation for equilibrium. Since fields do not change in equilibrium, any external supply such as r or production such as Joule's heat vanishes in equilibrium. In the most general case, we have to assume that the internal energy, heat flux, and electromagnetic polarization have reversible and irreversible parts. First, we assume that the internal energy is fully recoverable, neglecting the irreversible part of the internal energy. This is a conventional method that is appropriate for many engineering systems. We ignore effects of flux rates (the stress rate and heat flux rate) into the internal energy. For systems with high temperature rates or high velocity gradients, this method would be inaccurate and needs to be extended; see for example [39], [61]. The reversible part of the heat flux is given by a term called specific entropy, η, see ([32, Ch. XIV, §2])—this definition goes back to [18]—as follows

$$-\frac{\partial Q_i}{\partial X_i} = \rho_0 T \frac{\mathrm{d}\eta}{\mathrm{d}t} \ , \tag{68}$$

where we need a constitutive equation for the entropy. We neglect any hysteresis in the electromagnetic response and assume that electric and magnetic polarizations are reversible. In equilibrium, the balance of internal energy reads

$$\begin{aligned} \rho_0 \,\mathrm{d}u &= \rho_0 T \,\mathrm{d}\eta + N_{ji} \,\mathrm{d}F_{ij} - JP_i \,\mathrm{d}E_i + JB_i \,\mathrm{d}\mathcal{M}_i \ , \\ \mathrm{d}u &= T \,\mathrm{d}\eta + \frac{1}{\rho_0} N_{ji} \,\mathrm{d}F_{ij} - \frac{1}{\rho} P_i \,\mathrm{d}E_i + \frac{1}{\rho} B_i \,\mathrm{d}\mathcal{M}_i \ , \\ \mathrm{d}u &= T \,\mathrm{d}\eta + n_{ji} \,\mathrm{d}F_{ij} - p_i \,\mathrm{d}E_i + B_i \,\mathrm{d}\mathfrak{m}_i - B_i \mathcal{M}_i \,\mathrm{d}\mathrm{v} \ , \end{aligned} \tag{69}$$

where $p_i = P_i/\rho$ is the specific electric polarization in the current placement, $\mathfrak{m}_i = \mathcal{M}_i/\rho$ is the specific magnetic polarization in the current placement, $p = B_i\mathcal{M}_i$ is the electromagnetic pressure (owing to its unit), $\mathrm{v} = 1/\rho$ is the specific volume, and $n_{ji} = N_{ji}/\rho_0$ is the specific nominal stress in the initial placement. The last line can be called Gibbs's equation. It is a *perfect differential* that allows us to determine the internal energy by integrating its differential form. This assumption is called the first law of thermodynamics, see [70]. From the differential form, we immediately realize that the internal energy depends on $\{\eta, F_{ij}, E_i, \mathfrak{m}_i, \mathrm{v}\}$. Since we want to define η and $\mathfrak{m}_i$, it is beneficial to have a dependence on their conjugate variables, namely T and B_i. This is

achieved by introducing a free energy:

$$f = u - T\eta - B_i \mathit{m}_i \ , \tag{70}$$

and assuming that a perfect differential of this free energy exists such that

$$\begin{aligned} \mathrm{d}f &= \mathrm{d}u - \mathrm{d}T\eta - T\,\mathrm{d}\eta - \mathrm{d}B_i \mathit{m}_i - B_i\,\mathrm{d}\mathit{m}_i \ , \\ \mathrm{d}f &= -\eta\,\mathrm{d}T + n_{ji}\,\mathrm{d}F_{ij} - p_i\,\mathrm{d}E_i - \mathit{m}_i\,\mathrm{d}B_i - p\,\mathrm{dv} \ . \end{aligned} \tag{71}$$

The free energy depends on $\{T, F_{ij}, E_i, B_i, \mathrm{v}\}$. They can be called *primary* or *state* variables. We have the following obvious relations

$$\frac{\partial f}{\partial T} = -\eta \ , \quad \frac{\partial f}{\partial F_{ij}} = n_{ji} \ , \quad \frac{\partial f}{\partial E_i} = -p_i \ , \quad \frac{\partial f}{\partial B_i} = -\mathit{m}_i \ , \quad \frac{\partial f}{\partial \mathrm{v}} = -p = -B_i \mathcal{M}_i \ . \tag{72}$$

Additionally, because f depends on primary variables, each so-called *dual* variable, $\{\eta, n_{ji}, p_i, \mathit{m}_i, p\}$, depends on the same set of arguments—this is often named as equipresence principle, see [87, §293.η]—leading to

$$\begin{aligned} \mathrm{d}\eta &= \tilde{c}^{11}\,\mathrm{d}T + \tilde{c}^{12}_{kl}\,\mathrm{d}F_{kl} + \tilde{c}^{13}_{k}\,\mathrm{d}E_k + \tilde{c}^{14}_{k}\,\mathrm{d}B_k + \tilde{c}^{15}\,\mathrm{dv} \ , \\ \mathrm{d}n_{ji} &= \tilde{c}^{21}_{ji}\,\mathrm{d}T + \tilde{c}^{22}_{jikl}\,\mathrm{d}F_{kl} + \tilde{c}^{23}_{jik}\,\mathrm{d}E_k + \tilde{c}^{24}_{jik}\,\mathrm{d}B_k + \tilde{c}^{25}_{ji}\,\mathrm{dv} \ , \\ \mathrm{d}p_i &= \tilde{c}^{31}_{i}\,\mathrm{d}T + \tilde{c}^{32}_{ikl}\,\mathrm{d}F_{kl} + \tilde{c}^{33}_{ik}\,\mathrm{d}E_k + \tilde{c}^{34}_{ik}\,\mathrm{d}B_k + \tilde{c}^{35}_{i}\,\mathrm{dv} \ , \\ \mathrm{d}\mathit{m}_i &= \tilde{c}^{41}_{i}\,\mathrm{d}T + \tilde{c}^{42}_{ikl}\,\mathrm{d}F_{kl} + \tilde{c}^{43}_{ik}\,\mathrm{d}E_k + \tilde{c}^{44}_{ik}\,\mathrm{d}B_k + \tilde{c}^{45}_{i}\,\mathrm{dv} \ , \\ \mathrm{d}p &= \tilde{c}^{51}\,\mathrm{d}T + \tilde{c}^{52}_{kl}\,\mathrm{d}F_{kl} + \tilde{c}^{53}_{k}\,\mathrm{d}E_k + \tilde{c}^{54}_{k}\,\mathrm{d}B_k + \tilde{c}^{55}\,\mathrm{dv} \ . \end{aligned} \tag{73}$$

All material parameters, $\tilde{c}^{11}$, $\tilde{c}^{12}$, …, and $\tilde{c}^{55}$, need to be measured independently. There is a reduction of measurements due to the Maxwell symmetry relations (see Appendix D for their derivations). We can rewrite the above constitutive equations in the linear algebra fashion by using block matrices for the sake of clarity by

$$\begin{pmatrix} \mathrm{d}\eta \\ \mathrm{d}n_{ji} \\ \mathrm{d}p_i \\ \mathrm{d}\mathit{m}_i \\ \mathrm{d}p \end{pmatrix} = \begin{pmatrix} \tilde{c}^{11} & -\tilde{c}^{21}_{lk} & \tilde{c}^{31}_{k} & \tilde{c}^{41}_{k} & \tilde{c}^{51} \\ \tilde{c}^{21}_{ji} & \tilde{c}^{22}_{jikl} & -\tilde{c}^{32}_{kij} & -\tilde{c}^{42}_{kij} & -\tilde{c}^{52}_{ij} \\ \tilde{c}^{31}_{i} & \tilde{c}^{32}_{ikl} & \tilde{c}^{33}_{ik} & \tilde{c}^{43}_{ki} & \tilde{c}^{53}_{i} \\ \tilde{c}^{41}_{i} & \tilde{c}^{42}_{ikl} & \tilde{c}^{43}_{ik} & \tilde{c}^{44}_{ik} & \tilde{c}^{54}_{i} \\ \tilde{c}^{51} & \tilde{c}^{52}_{kl} & \tilde{c}^{53}_{k} & \tilde{c}^{54}_{k} & \tilde{c}^{55} \end{pmatrix} \begin{pmatrix} \mathrm{d}T \\ \mathrm{d}F_{kl} \\ \mathrm{d}E_k \\ \mathrm{d}B_k \\ \mathrm{dv} \end{pmatrix} . \tag{74}$$

The experiments to determine these coefficients are established by varying a primary variable while holding all other primary variables constant and measuring one dual variable. Consider the first dual variable: instead of measuring entropy, we observe the heat flux $\delta Q = T\,\mathrm{d}\eta$ and then measure temperature by holding the deformation gradient, electromagnetic fields, and mass density fixed at a specific value such that their variations are zero, i.e., $\mathrm{d}F_{kl} = 0$, $\mathrm{d}E_i = 0$, $\mathrm{d}B_i = 0$, $\mathrm{dv} = 0$. The parameter c relating heat flux to temperature is called the specific heat capacity, $\delta Q = c\,\mathrm{d}T$, so we obtain $\tilde{c}^{11} = c/T$. Heat capacity can depend on fields besides the temperature. The specific stiffness[1] tensor, $\tilde{c}^{22}_{jikl}$, is measured for a specifically chosen state of a held temperature, electromagnetic fields, and mass density and then applying a deformation and measuring stress. All other coefficients can be measured in analogous settings. For example $\tilde{c}^{33}_{ik}$ and $\tilde{c}^{44}_{ik}$ are susceptibilities. Between the electromagnetic pressure p and specific volume v, the coefficient $\tilde{c}^{55}$ can be measured by applying magnetic field and measuring the volume change. Such measurements are very challenging, but possible. Moreover, the off-diagonal terms are different coupling terms between primary variables. For example, $\tilde{c}^{23}_{jik}$ and $\tilde{c}^{24}_{jik}$ are coupling stress with electromagnetic fields, called the specific piezoelectric and piezomagnetic material coefficients, respectively.

Finding the suggested coefficients in the literature is challenging due to difficulties in making the described measurements. Hence, we will switch to quantities that are more regularly measured and thus appear more frequently in the literature. Coefficients of thermal expansion, α_{ij}, are measured by varying temperature and measuring length change

$$\mathrm{d}F_{ij} = \alpha_{ij}\,\mathrm{d}T \ , \tag{75}$$

[1] Note that this stiffness tensor is not the stiffness tensor which is normally discussed. In our derivation, we have a stiffness tensor to be the derivative of a non-symmetric tensor with respect to another non-symmetric tensor. Thus, the minor symmetries are not present. Further, since we never declared a quadratic strain energy function, the major symmetry is also not necessarily present. The symmetry relations are introduced as a consequence of any existing crystal symmetries. For example, in the case of an isotropic material, all aforementioned symmetries arise.

by holding every other variable fixed such that we acquire from Eq. $(74)_{2,3,4,5}$ the following relations

$$\begin{aligned}
0 &= \tilde{c}^{21}_{ji}\,\mathrm{d}T + \tilde{c}^{22}_{jikl}\alpha_{kl}\,\mathrm{d}T \Rightarrow \tilde{c}^{21}_{ji} = -\tilde{c}^{22}_{jikl}\alpha_{kl}\ , \\
0 &= \tilde{c}^{31}_{i}\,\mathrm{d}T + \tilde{c}^{32}_{ikl}\alpha_{kl}\,\mathrm{d}T \Rightarrow \tilde{c}^{31}_{i} = -\tilde{c}^{32}_{ikl}\alpha_{kl}\ , \\
0 &= \tilde{c}^{41}_{i}\,\mathrm{d}T + \tilde{c}^{42}_{ikl}\alpha_{kl}\,\mathrm{d}T \Rightarrow \tilde{c}^{41}_{i} = -\tilde{c}^{42}_{ikl}\alpha_{kl}\ , \\
0 &= \tilde{c}^{51}\,\mathrm{d}T + \tilde{c}^{52}_{kl}\alpha_{kl}\,\mathrm{d}T \Rightarrow \tilde{c}^{51} = -\tilde{c}^{52}_{kl}\alpha_{kl}\ .
\end{aligned} \tag{76}$$

For simplicity we present the case, where material coefficients are constants in the corresponding variable of integration: c is constant in T and $\tilde{c}^{22}_{jikl}$ is constant in F_{ij} and so on. In this case, we can easily integrate from a reference state $T = T_{\mathrm{ref.}}$, $F_{ij} = \delta_{ij}$, $E_i = 0$, $B_i = 0$, and $\mathrm{v} = \mathrm{v}_{\mathrm{ref.}}$ to the current state. We define the reference state as the state in which all dual variables vanish. After integrating and multiplying by mass density, we obtain the relations

$$\begin{aligned}
\eta &= c\ln\Big(\frac{T}{T_{\mathrm{ref.}}}\Big) + \tilde{c}^{22}_{lkij}\alpha_{ij}(F_{kl}-\delta_{kl}) - \tilde{c}^{32}_{kij}\alpha_{ij}E_k - \tilde{c}^{42}_{kij}\alpha_{ij}B_k - \tilde{c}^{52}_{ij}\alpha_{ij}(\mathrm{v}-\mathrm{v}_{\mathrm{ref.}})\ , \\
N_{ji} &= -\rho_0\tilde{c}^{22}_{jikl}\alpha_{kl}(T-T_{\mathrm{ref.}}) + \rho_0\tilde{c}^{22}_{jikl}(F_{kl}-\delta_{kl}) - \rho_0\tilde{c}^{32}_{kij}E_k - \rho_0\tilde{c}^{42}_{kij}B_k - \rho_0\tilde{c}^{52}_{ij}(\mathrm{v}-\mathrm{v}_{\mathrm{ref.}})\ , \\
P_i &= -\rho\tilde{c}^{32}_{ikl}\alpha_{kl}(T-T_{\mathrm{ref.}}) + \rho\tilde{c}^{32}_{ikl}(F_{kl}-\delta_{kl}) + \rho\tilde{c}^{33}_{ik}E_k + \rho\tilde{c}^{43}_{ki}B_k + \rho\tilde{c}^{53}_{i}(\mathrm{v}-\mathrm{v}_{\mathrm{ref.}})\ , \\
\mathcal{M}_i &= -\rho\tilde{c}^{42}_{ikl}\alpha_{kl}(T-T_{\mathrm{ref.}}) + \rho\tilde{c}^{42}_{ikl}(F_{kl}-\delta_{kl}) + \rho\tilde{c}^{43}_{ik}E_k + \rho\tilde{c}^{44}_{ik}B_k + \rho\tilde{c}^{54}_{i}(\mathrm{v}-\mathrm{v}_{\mathrm{ref.}})\ , \\
p &= -\tilde{c}^{52}_{kl}\alpha_{kl}(T-T_{\mathrm{ref.}}) + \tilde{c}^{52}_{kl}(F_{kl}-\delta_{kl}) + \tilde{c}^{53}_{k}E_k + \tilde{c}^{54}_{k}B_k + \tilde{c}^{55}(\mathrm{v}-\mathrm{v}_{\mathrm{ref.}})\ .
\end{aligned} \tag{77}$$

The reference temperature $T_{\mathrm{ref.}}$ as well as the specific volume $\mathrm{v}_{\mathrm{ref.}}$ need to be specified. Although these values are material specific, we assume that the initial mass density and temperature can be chosen as reference values. In other words, we start simulating from the ground state without entropy, stress, and polarization. Since the deformation gradient is the sum of identity and displacement gradient, we have $\partial u_i/\partial X_j = F_{ij} - \delta_{ij}$. It is important to mention that we use $\partial u_i/\partial X_j$ instead of strain, since the additional term in the nominal stress fail to be symmetric. The mechanical part of the nominal stress (transpose of the Piola stress) relates the current force to initial area and it is often called the *engineering* stress. In an experiment, the length change is recorded and often the so-called *engineering* strain is reported as current length (measured length change plus initial length) divided by the initial length, which is one component of F_{ij}. Hence, we can use the reported stiffness values in $\tilde{c}^{22}_{ijkl}$. For the thermodynamic analysis we have used specific variables; however, in reality the measurements are established utilizing stress and polarization, N_{ji}, P_i, $\mathcal{M}_i$, instead of their per mass values, n_{ji}, p_i, $\mathfrak{m}_i$. Therefore, we rename the material coefficients as follows

$$\begin{aligned}
\rho_0\tilde{c}^{22}_{jikl} &= C_{jikl}\ , \quad \rho_0\tilde{c}^{32}_{kij} = \tilde{T}_{kij}\ , \quad \rho_0\tilde{c}^{42}_{kij} = \tilde{S}_{kij}\ , \\
\rho\tilde{c}^{33}_{ik} &= \varepsilon_0\chi^{\mathrm{el.}}_{ik}\ , \quad \rho\tilde{c}^{43}_{ki} = \tilde{R}_{ki}\ , \quad \rho\tilde{c}^{44}_{ik} = (\boldsymbol{\mu}^{-1}_{\mathrm{mag.}})_{ij}\chi^{\mathrm{mag.}}_{jk}\ .
\end{aligned} \tag{78}$$

As we have used the electromagnetic pressure (energy density) $p = \mathcal{M}_i B_i$ we obtain by multiplying $\mathcal{M}_i$ by B_i and matching the coefficients to p,

$$\begin{aligned}
\tilde{c}^{52}_{kl} &= \rho\tilde{c}^{42}_{ikl}B_i = J^{-1}\tilde{S}_{ikl}B_i\ , \quad \tilde{c}^{53}_{k} = \rho\tilde{c}^{43}_{ik}B_i = \tilde{R}_{ik}B_i\ , \\
\tilde{c}^{54}_{k} &= \rho\tilde{c}^{44}_{ik}B_i = (\boldsymbol{\mu}^{-1}_{\mathrm{mag.}})_{ij}\chi^{\mathrm{mag.}}_{jk}B_i\ , \quad \tilde{c}^{55}_{k} = \rho\tilde{c}^{54}_{i}B_i\ .
\end{aligned} \tag{79}$$

Finally, we acquire the following constitutive equations

$$\begin{aligned}
\eta &= c\ln\Big(\frac{T}{T_{\mathrm{ref.}}}\Big) + \mathrm{v}_0 C_{lkij}\alpha_{ij}\frac{\partial u_k}{\partial X_l} - \mathrm{v}_0\tilde{T}_{kij}\alpha_{ij}E_k - \mathrm{v}_0(2-J^{-1})\tilde{S}_{kij}\alpha_{ij}B_k\ , \\
N_{ji} &= C_{jikl}\Big(-\alpha_{kl}(T-T_{\mathrm{ref.}}) + \frac{\partial u_k}{\partial X_l}\Big) - \tilde{T}_{kij}E_k - (2-J^{-1})\tilde{S}_{kij}B_k\ , \\
P_i &= J^{-1}\tilde{T}_{ikl}\Big(-\alpha_{kl}(T-T_{\mathrm{ref.}}) + \frac{\partial u_k}{\partial X_l}\Big) + \varepsilon_0\chi^{\mathrm{el.}}_{ik}E_k + (2-J^{-1})\tilde{R}_{ki}B_k\ , \\
\mathcal{M}_i &= J^{-1}\tilde{S}_{ikl}\Big(-\alpha_{kl}(T-T_{\mathrm{ref.}}) + \frac{\partial u_k}{\partial X_l}\Big) + \tilde{R}_{ik}E_k + (2-J^{-1})(\boldsymbol{\mu}^{-1}_{\mathrm{mag.}})_{ij}\chi^{\mathrm{mag.}}_{jk}B_k\ .
\end{aligned} \tag{80}$$

Especially, the stiffness tensor C_{ijkl}, electric susceptibility $\chi^{\mathrm{el.}}_{ij}$, magnetic susceptibility $\chi^{\mathrm{mag.}}_{ij}$, permeability of the vacuum ε_0, permittivity of the material μ_{ij} are available for many engineering materials. Piezoelectric and piezomagnetic coefficients, $\tilde{T}_{ijk}$ and $\tilde{S}_{ijk}$, are also possible to find. Often, as stated in [56], the measurements

are undertaken by varying electric field and measuring displacement gradient, $\mathrm{d}\partial u_i/\partial X_j = d_{kij}\,\mathrm{d}E_k$, and by determining d_{kij} with the standard notation. In this case, we can readily find from Eq. $(74)_2$ the relation

$$\tilde{T}_{mij} = C_{ijkl} d_{mkl} \ . \tag{81}$$

Also quite often, the piezomagnetic constants are given in $\mathrm{T}\hat{=}\mathrm{N}/(\mathrm{A\,m})$ as $\tilde{q}_{ijk} = \mu_0 \tilde{S}_{ijk}$. The magnetoelectric coupling $\tilde{R}_{ij}$ is rarely measured.

For the case of nonlinear material equations, the functional form of the coefficients need to be known for the integration. In a slightly abusive notation we can include the nonlinear materials, for example for hyperelasticity C_{jikl} depends on F_{ij} and by recalling

$$\frac{\partial f}{\partial F_{ij}} = n_{ji} \ , \quad \frac{\partial n_{ji}}{\partial F_{kl}} = \tilde{c}^{22}_{jikl} \ , \quad \rho_0 \tilde{c}^{22}_{jikl} = C_{jikl} \ , \quad \frac{\partial n_{ji}}{\partial B_k} = \tilde{c}^{24}_{jik} = -\tilde{c}^{42}_{kij} \ , \quad \rho_0 \tilde{c}^{42}_{kij} = \tilde{S}_{kij} \ , \tag{82}$$

we obtain

$$C_{jikl} = \rho_0 \frac{\partial^2 f}{\partial F_{ij} \partial F_{kl}} \ , \quad \tilde{S}_{kij} = -\rho_0 \frac{\partial^2 f}{\partial B_k \partial F_{ij}} \ . \tag{83}$$

Especially for soft materials the measurement of the free energy is more feasible than the stiffness tensor, see [86]. For the case of an isotropic material, the free energy fail to depend on the material frame, thus, free energy's dependency on the deformation gradient can be given by means of the invariants. From the thermodynamics point of view, any function can be suggested as a material equation. Yet there are some restrictions because of the approximative computation in a weak form, these are called *ellipticity*—in the special case of an isotropic material, *invertibility*—in order to assure a smooth deformation gradient, $[\![\boldsymbol{F}]\!] = 0$, within the computational domain, see [76]. For the isotropic case, the dependency is given by invariants instead of a single argument $\boldsymbol{F}$. Then ellipticity holds in every single argument of the free energy, and this case is called *quasiconvexity*. The choice of the functional form and the material constants shall not violate the quasiconvexity in order to compute the primitive variables with sufficient smoothness.

Since we have now defined all necessary constitutive equations, we insert Gibbs's equation in the balance of internal energy to acquire

$$\rho_0 T \frac{\partial \eta}{\partial t} = -\frac{\partial Q_j}{\partial X_j} + \rho_0 r + J \mathcal{E}_i \jmath_i^{\mathrm{fr.}} \ , \tag{84}$$

emphasizing that we have assumed elasticity and no dissipation in polarization. With a slight rearrangement we obtain the balance of entropy:

$$\rho_0 \frac{\partial \eta}{\partial t} + \frac{\partial}{\partial X_j}\Big(\frac{Q_j}{T}\Big) - \rho_0 \frac{r}{T} = -\frac{Q_j}{T^2}\frac{\partial T}{\partial X_j} + \frac{J}{T}\mathcal{E}_i \jmath_i^{\mathrm{fr.}} \tag{85}$$

The entropy flux can differ from this formulation if the energy flux in Eq. (42) is defined differently. A well-known alternative includes the term $\boldsymbol{E} \times \boldsymbol{\mathfrak{H}}$ into the heat flux. In this formulation, the entropy flux and production would have an additional term in the heat flux similar to a Hall effect; for its elaborate discussion see [60, §9.9.4]. We continue by using the chosen definition leading to the usual definition as above and declare the thermodynamical fluxes $-Q_i$ and $\jmath_i^{\mathrm{fr.}}$ to depend on the thermodynamical forces $T^{-2}\partial T/\partial X_i$ and $JT^{-1}\mathcal{E}_i$. By using representation theorems, we can determine the following functional relationships

$$-Q_i = \tilde{k}^{11} T^{-2} \frac{\partial T}{\partial X_i} + \tilde{k}^{12} J T^{-1} \mathcal{E}_i \ , \quad \jmath_i^{\mathrm{fr.}} = \tilde{k}^{21} T^{-2} \frac{\partial T}{\partial X_i} + \tilde{k}^{22} J T^{-1} \mathcal{E}_i \ . \tag{86}$$

According to the second law of thermodynamics, the entropy production has to be positive for any process, i.e.,

$$\tilde{k}^{11} T^{-4} \frac{\partial T}{\partial X_i}\frac{\partial T}{\partial X_i} + (\tilde{k}^{12} + \tilde{k}^{21}) J T^{-3} \mathcal{E}_i \frac{\partial T}{\partial X_i} + \tilde{k}^{22} J T^{-1} \mathcal{E}_i \mathcal{E}_i \geq 0 \tag{87}$$

such that we obtain the restrictions

$$\tilde{k}^{11} \geq 0 \ , \quad \tilde{k}^{12} + \tilde{k}^{21} = 0 \ , \quad \tilde{k}^{22} \geq 0 \ , \tag{88}$$

since the absolute temperature is positive, $T > 0$, and the determinant of the deformation gradient is positive, $J > 0$. The coefficients, $\tilde{k}^{\times\times}$, are scalar functions depending on the invariants of temperature gradient and

electric field. For the simplified case of constant coefficients, the above linear relations can be derived by using statistical mechanics, where the second restriction $\tilde{k}^{12} = -\tilde{k}^{21}$ is named after Onsager. For showing the relevance to well-established phenomenological equations, we rename the material parameters

$$\kappa = \tilde{k}^{11} T^{-2} \ , \quad \varsigma = \tilde{k}^{22} J T^{-1} \ , \quad \varsigma\pi = -\tilde{k}^{12} T^{-2} \ , \tag{89}$$

and obtain the following constitutive equations:

$$Q_i = -\kappa \frac{\partial T}{\partial X_i} + \varsigma\pi T J \mathcal{E}_i \ , \quad \mathcal{J}_i^{\text{fr.}} = \varsigma\pi \frac{\partial T}{\partial X_i} + \varsigma \mathcal{E}_i \ . \tag{90}$$

The heat conduction coefficient, κ, electrical conductivity, ς, and the thermoelectric coupling coefficient, π, are determined experimentally. The thermoelectric coupling is found to be constant for many engineering materials. Often it is called the Peltier constant. Although every conducting material possesses a Peltier constant, it might be small enough to be ignored. For the case of $\kappa = \text{const.}$ and $\pi = 0$, the constitutive equation for the heat flux is called Fourier's law. For the case of $\varsigma = \text{const.}$ and $\pi = 0$, the constitutive equation for the electric current is named after Ohm.

4. Computational approach

A considerable amount of studies and efforts are undertaken for solving mechanics and electromagnetism. For thermomechanics, we may claim the finite element method (FEM) with Galerkin approach using standard (continuous piecewise polynomials called $\mathcal{P}_n$ elements) n-times differential elements is *the gold standard*. If it comes to electromagnetism, there are several methods among scientists—for example see [13], [20], [21, Sect. 17], [45], [25], [2], [27]—and a consensus is yet missing. If one aims at solving electromagnetic fields $\boldsymbol{E}$ and $\boldsymbol{B}$ by satisfying Maxwell's equations, then FEM with standard elements cannot be used and there are various so-called mixed elements, see [5], whose techniques are based on works of [74] and [63]. Very roughly summarized, the mixed elements possess special forms for the functions fulfilling two of Maxwell's equations. From a theoretical point of view, this method is correct since the ultimate goal is to compute the electromagnetic fields directly.

As we have seen in the formulation, the introduction of electromagnetic potentials, ϕ and $\boldsymbol{A}$, simplifies the procedure by solving two of Maxwell's equations in a closed form. As a consequence, we can set the objective to compute the electromagnetic potentials by means of standard elements, as successfully applied in [1, Chap. 3]. After computing electromagnetic potentials, we can easily derive the electromagnetic fields by post-processing the solution with the equations

$$E_i = -\frac{\partial \phi}{\partial x_i} - \frac{\partial A_i}{\partial t} \ , \quad B_i = \epsilon_{ijk} \frac{\partial A_k}{\partial x_j} \ , \tag{91}$$

where $\boldsymbol{x}$ denotes the coordinate in the Eulerian frame; i.e., the derivatives $\partial/\partial t$ and $\partial/\partial x_i$ are taken with respect to the spatial position in the laboratory frame. The space in this frame will be discretized for the computation by using standard triangulation/tetrahedralization methods. The nodes possess coordinates in the laboratory frame. However, the nodes can move with an arbitrary velocity $\boldsymbol{w}$ which we call the domain or mesh velocity and emphasize that it is arbitrary. In order to satisfy Eq. (58), we choose $\boldsymbol{w}$ based on the motion of the continuum body. All script values, $\boldsymbol{\mathcal{D}}$, $\boldsymbol{\mathcal{H}}$, $\boldsymbol{\mathcal{E}}$, and $\boldsymbol{\mathcal{B}}$ are measured in the moving domain. We will use their counterparts $\boldsymbol{D}$, $\boldsymbol{H}$, $\boldsymbol{E}$, and $\boldsymbol{B}$ in the laboratory frame (as a coincidence $\boldsymbol{\mathcal{D}} = \boldsymbol{D}$ and $\boldsymbol{\mathcal{B}} = \boldsymbol{B}$). The electromagnetic potentials ϕ and $\boldsymbol{A}$ are calculated by fulfilling the governing Eqs. (21) with the total charge:

$$\begin{aligned} J_i &= \mathcal{J}_i^{\text{fr.}} + q^{\text{fr.}} v_i + \frac{\partial P_i}{\partial t} + \epsilon_{ijk} \frac{\partial \mathcal{M}_k}{\partial x_j} \ , \quad q^{\text{fr.}} = \frac{\partial \mathfrak{D}_i}{\partial x_i} \ , \\ D_i &= \varepsilon_0 E_i \ , \quad H_i = \frac{1}{\mu_0} B_i \ , \quad \mathfrak{D}_i = D_i + P_i \ , \quad \mathfrak{H}_i = H_i - \mathcal{M}_i \ , \end{aligned} \tag{92}$$

as well as the material specific relations:

$$\begin{aligned} \mathcal{J}_i^{\text{fr.}} &= \varsigma\pi\frac{\partial T}{\partial X_i} + \varsigma\mathcal{E}_i \ , \\ P_i &= J^{-1}\tilde{T}_{ikl}\Big(- \alpha_{kl}(T - T_{\text{ref.}}) + \frac{\partial u_k}{\partial X_l}\Big) + \varepsilon_0\chi^{\text{el.}}_{ik}E_k + (2 - J^{-1})\tilde{R}_{ki}B_k \ , \\ \mathcal{M}_i &= J^{-1}\tilde{S}_{ikl}\Big(- \alpha_{kl}(T - T_{\text{ref.}}) + \frac{\partial u_k}{\partial X_l}\Big) + \tilde{R}_{ik}E_k + (2 - J^{-1})(\boldsymbol{\mu}^{-1}_{\text{mag.}})_{ij}\chi^{\text{mag.}}_{jk}B_k \ , \end{aligned} \tag{93}$$

where the differentiation in space occurs in the LAGRANGEan frame in coordinates $\boldsymbol{X}$, which can be visualized as moving with the material velocity $v_i = \partial u_i/\partial t$. The displacement, $\boldsymbol{u}$, and temperature, T, as well as their gradients are computed in the LAGRANGEan frame. For example, $\partial u_i/\partial X_j$ is computed in the LAGRANGEan frame and then mapped to the EULERian frame by projecting this tensor to each coordinate $\boldsymbol{x}$. Deformation is obtained by fulfilling the balance of momentum

$$\rho_0\frac{\partial^2 u_i}{\partial t^2} = \frac{\partial}{\partial X_k}\Big(J(\boldsymbol{F}^{-1})_{kj}\sigma_{ji}\Big) + \rho_0 f_i + J\mathcal{F}_i \tag{94}$$

by using the displacement $\boldsymbol{u}$ as a function in the initial placement. Initial mass density, ρ_0, is a given constant for a homogeneous material and is a known function in $\boldsymbol{X}$ for a heterogeneous material, and so is the specific body force due to the gravitation, $\boldsymbol{f}$. The electromagnetic force density in the LAGRANGEan frame reads

$$J\mathcal{F}_i = JqE_i + J\epsilon_{ijk}J_jB_k - J\epsilon_{ijk}\frac{\partial P_j}{\partial t}B_k - J\epsilon_{ijk}P_j\frac{\partial B_k}{\partial t} \ , \tag{95}$$

where this time $q = \partial D_i/\partial x_i$, B_i and E_i from Eq. (91) are computed in the EULERian frame and projected to the LAGRANGEan frame as scalar, vectors, respectively. The stress,

$$\begin{aligned} \sigma_{ji} &= J^{-1}F_{jk}N_{ki} + P_jE_i - \mathcal{M}_iB_j \ , \\ N_{ji} &= C_{jikl}\Big(- \alpha_{kl}(T - T_{\text{ref.}}) + \frac{\partial u_k}{\partial X_l}\Big) - \tilde{T}_{kij}E_k - (2 - J^{-1})\tilde{S}_{kij}B_k \ , \end{aligned} \tag{96}$$

has been derived such that Eq. (94) is closed and can be solved. Temperature, T, can either be solved by using the balance of internal energy or the balance of entropy. We use the latter

$$\rho_0\frac{\partial \eta}{\partial t} + \frac{\partial}{\partial X_j}\Big(\frac{Q_j}{T}\Big) - \rho_0\frac{r}{T} = -\frac{Q_j}{T^2}\frac{\partial T}{\partial X_j} + \frac{J}{T}\mathcal{E}_i\mathcal{J}_i^{\text{fr.}} \ , \tag{97}$$

by closing it with the following constitutive equations

$$\begin{aligned} \eta &= c\ln\Big(\frac{T}{T_{\text{ref.}}}\Big) + \mathrm{v}_0C_{lkij}\alpha_{ij}\frac{\partial u_k}{\partial X_l} - \mathrm{v}_0\tilde{T}_{kij}\alpha_{ij}E_k - \mathrm{v}_0(2 - J^{-1})\tilde{S}_{kij}\alpha_{ij}B_k \ , \\ Q_i &= -\kappa\frac{\partial T}{\partial X_i} + \varsigma\pi TJ\mathcal{E}_i \ . \end{aligned} \tag{98}$$

The governing equations will be rewritten as integral forms leading to a nonlinear and coupled weak form. This nonlinear and coupled weak form will be solved numerically.

4.1. Variational formulation

The whole computational domain is divided into non-overlapping finite elements with compact support. This discrete representation of the domain allows us to fulfill governing equations in finite elements. The equations are written as residuals and multiplied by a suitable test function in order to obtain scalar functions, which are then integrated over a finite element. This procedure is often called the variational formulation.[2] Within the finite element, the fields are n-times continuous and we will use standard Lagrange polynomial tetrahedral elements of order one such that their first derivative in space exists. All analytic fields are represented by discrete functions, and so we omit a notational indication for the discrete functions. For the discretization in time, we use the backward EULER method since it is an implicit L-stable method. For every partial time derivative, we

[2] Actually, the variational formulation is a terminology to be used if one starts with action and obtains the same integral form by taking its first variation. Since the outcome is identical, we use the same wording.

apply

$$\frac{\partial(\cdot)}{\partial t} = \frac{(\cdot) - (\cdot)^0}{\Delta t} \ , \tag{99}$$

where the superscript 0 denotes the value at the previous timestep. For second derivatives in time, we combine estimates of the first derivative at the current timestep and previous timestep to obtain

$$\frac{\partial^2(\cdot)}{\partial t^2} = \frac{(\cdot) - 2(\cdot)^0 + (\cdot)^{00}}{\Delta t \Delta t} \ , \tag{100}$$

where the superscript 00 denotes the value two timesteps ago. Thus, in our scheme, we solve the systems of equations for the current field value at t while using the previous values at $t - \Delta t$ ("0") and $t - 2\Delta t$ ("00").

We begin formulating the variational form to solve the electromagnetic fields as computed in the current placement. The governing Eqs. (21) as residuals read

$$\frac{\partial q}{\partial t} + \frac{\partial J_i}{\partial x_i} = 0 \ , \quad \frac{\partial D_j}{\partial t} - \epsilon_{jki} \frac{\partial H_i}{\partial x_k} + J_j = 0 \ . \tag{101}$$

The first scalar equation will deliver the scalar potential, ϕ, and the second vector equations will serve for the vector potential, $\boldsymbol{A}$. By utilizing the variational formulation, we acquire the integral form,

$$\int_\Omega \left(\frac{q - q^0}{\Delta t} + \frac{\partial J_i}{\partial x_i} \right) \delta\phi \, \mathrm{d}v = 0 \ . \tag{102}$$

We multiply the form by Δt in order to bring it to the unit of energy. Moreover, we observe the derivative of the electric current, which includes $\boldsymbol{E}$ depending on the derivative of ϕ. Therefore, the unknown ϕ has to be twice differentiable. Same holds for q including the derivative of $\boldsymbol{D}$ depending on $\boldsymbol{E}$. This condition is weakened by integrating by parts, leading to the so-called weak form:

$$\mathrm{F}_\phi = \int_\Omega \left(- (D_i - D_i^0) - \Delta t J_i \right) \frac{\partial \delta\phi}{\partial x_i} \, \mathrm{d}v + \int_{\partial\Omega} n_i (D_i - D_i^0 + \Delta t J_i) \delta\phi \, \mathrm{d}a \ , \tag{103}$$

where $\boldsymbol{n}$ is the unit normal on the element surface. If we sum up over all elements, which is called *assembly* then the weak form becomes

$$\begin{aligned} \mathrm{F}_\phi = \sum_{\text{ele.}} \int_\Omega \left(- (D_i - D_i^0) - \Delta t J_i \right) \frac{\partial \delta\phi}{\partial x_i} \, \mathrm{d}v + \sum_{\text{sur.}} \int_{\partial\Omega} \left[\!\left[n_i (D_i - D_i^0 + \Delta t J_i) \delta\phi \right]\!\right] \mathrm{d}a + \\ + \sum_{\text{outer}} \int_{\partial\Omega} n_i (D_i - D_i^0 + \Delta t J_i) \delta\phi \, \mathrm{d}a \ . \end{aligned} \tag{104}$$

Three distinct summations are applied: summation over the elements, summation over the inner surfaces with two adjacent elements, and summation over the outer surfaces being on the computational domain boundary. The computational domain is a sphere including the continuum body such that the computational domain boundary represents the far away boundaries, where electromagnetic potentials vanish. We set ϕ at the computational domain via Dirichlet boundary condition such that its test function on the outer $\partial\Omega$ vanishes. For the term in jump brackets we use Eqs. (61) as follows

$$\left[\!\left[n_i (D_i - D_i^0 + \Delta t J_i) \delta\phi \right]\!\right] = \left[\!\left[n_i \Big(\Delta t J_i^{\text{fr.}} + P_i - P_i^0 + \Delta t \epsilon_{ijk} \frac{\partial \mathcal{M}_k}{\partial x_j} \Big) \delta\phi \right]\!\right] = \left[\!\left[n_i \Delta t \Big(J_i^{\text{fr.}} + \epsilon_{ijk} \frac{\partial \mathcal{M}_k}{\partial x_j} \Big) \delta\phi \right]\!\right] \ . \tag{105}$$

Finally, we obtain the weak form for computing the electric potential in the Eulerian frame,

$$\mathrm{F}_\phi = \sum_{\text{ele.}} \int_\Omega \left(- (D_i - D_i^0) - \Delta t J_i \right) \frac{\partial \delta\phi}{\partial x_i} \, \mathrm{d}v + \sum_{\text{sur.}} \int_{\partial\Omega} \left[\!\left[n_i \Delta t \Big(J_i^{\text{fr.}} + \epsilon_{ijk} \frac{\partial \mathcal{M}_k}{\partial x_j} \Big) \delta\phi \right]\!\right] \mathrm{d}a \ . \tag{106}$$

To improve the numerical stability, we rewrite the second equation by inserting the Maxwell–Lorentz aether

relations and then the electromagnetic potentials from Eq. (8) as follows

$$\begin{aligned}
\frac{\partial \varepsilon_0 E_j}{\partial t} - \epsilon_{jki}\frac{\partial}{\partial x_k}\Big(\frac{1}{\mu_0}B_i\Big) + J_j = 0 \ , \\
-\varepsilon_0\frac{\partial^2\phi}{\partial t \partial x_j} - \varepsilon_0\frac{\partial^2 A_j}{\partial t^2} - \frac{1}{\mu_0}\epsilon_{jki}\epsilon_{ilm}\frac{\partial^2 A_m}{\partial x_k \partial x_l} + J_j = 0 \ , \\
-\frac{\partial}{\partial x_j}\Big(\varepsilon_0\frac{\partial\phi}{\partial t} + \frac{1}{\mu_0}\frac{\partial A_k}{\partial x_k}\Big) - \varepsilon_0\frac{\partial^2 A_j}{\partial t^2} + \frac{1}{\mu_0}\frac{\partial^2 A_j}{\partial x_k \partial x_k} + J_j = 0 \ ,
\end{aligned} \tag{107}$$

since $\epsilon_{jki}\epsilon_{ilm} = \delta_{jl}\delta_{km} - \delta_{jm}\delta_{kl}$. The first term in brackets vanishes as a consequence of LORENZ's gauge in Eq. (9). Then the variational formulation delivers

$$\begin{aligned}
\int_\Omega \Big(-\varepsilon_0\frac{A_j - 2A_j^0 + A_j^{00}}{\Delta t \Delta t} + \frac{1}{\mu_0}\frac{\partial^2 A_j}{\partial x_k \partial x_k} + J_j\Big)\delta A_j \,\mathrm{d}v = 0 \ , \\
\mathrm{F}_{\boldsymbol{A}} = \int_\Omega \Big(-\varepsilon_0\frac{A_j - 2A_j^0 + A_j^{00}}{\Delta t \Delta t}\delta A_j - \frac{1}{\mu_0}\frac{\partial A_j}{\partial x_k}\frac{\partial \delta A_j}{\partial x_k} + J_j^{\mathrm{fr.}}\delta A_j + \frac{P_j - P_j^0}{\Delta t}\delta A_j - \\
-\epsilon_{jki}\mathcal{M}_i\frac{\partial \delta A_j}{\partial x_k}\Big)\,\mathrm{d}v + \int_{\partial\Omega}\Big(\frac{1}{\mu_0}\frac{\partial A_j}{\partial x_k} + \epsilon_{jki}\mathcal{M}_i\Big)\delta A_j n_k \,\mathrm{d}a \ ,
\end{aligned} \tag{108}$$

after an integration by parts on the terms already including a derivative. The integral form is in the unit of energy. The assembly generates a jump term,

$$\Big[\!\Big[\Big(\frac{1}{\mu_0}\frac{\partial A_j}{\partial x_k} + \epsilon_{jki}\mathcal{M}_i\Big)\delta A_j n_k\Big]\!\Big] \ , \tag{109}$$

which vanishes by using Eqs. (61), (63). Moreover, we set the magnetic potential zero at the computational domain boundary. Hence, the weak form for the magnetic potential reads in the EULERian frame,

$$\mathrm{F}_{\boldsymbol{A}} = \sum_{\mathrm{ele.}}\int_\Omega \Big(-\varepsilon_0\frac{A_j - 2A_j^0 + A_j^{00}}{\Delta t \Delta t}\delta A_j - \frac{1}{\mu_0}\frac{\partial A_j}{\partial x_k}\frac{\partial \delta A_j}{\partial x_k} + J_j^{\mathrm{fr.}}\delta A_j + \frac{P_j - P_j^0}{\Delta t}\delta A_j - \epsilon_{jki}\mathcal{M}_i\frac{\partial \delta A_j}{\partial x_k}\Big)\,\mathrm{d}v \ . \tag{110}$$

In the case of thermomechanics, we solve T and u_i in the LAGRANGEan frame. With the variational formulation discrete in time and after integrating by parts, the balance of linear momentum reads

$$\mathrm{F}_{\boldsymbol{u}} = \int_{\mathcal{B}_0}\Big(\rho_0\frac{u_i - 2u_i^0 + u_i^{00}}{\Delta t \Delta t}\delta u_i + J(\boldsymbol{F}^{-1})_{kj}\sigma_{ji}\frac{\partial \delta u_i}{\partial X_k} - \rho_0 f_i \delta u_i - J\mathcal{F}_i\delta u_i\Big)\,\mathrm{d}V - \int_{\partial\mathcal{B}_0} J(\boldsymbol{F}^{-1})_{kj}\sigma_{ji}\delta u_i N_k \,\mathrm{d}A \ , \tag{111}$$

where we distinguish between the infinitesimal elements, plane normals, as well as domains in the LAGRANGEan and EULERian frames for the sake of clarity. The latter integral form is in the unit of energy. The assembly results in a vanishing jump term in connection with Eq. (58). On the boundaries, where the boundary for the thermomechanics means the interface to the surrounding air, either we set the displacements by using DIRICHLET condition or set the applied traction force per area $\hat{t}_i = N_k J(\boldsymbol{F}^{-1})_{kj}\sigma_{ji}$ by using NEUMANN condition. The weak form for computing the displacement reads

$$\mathrm{F}_{\boldsymbol{u}} = \sum_{\mathrm{ele.}}\int_{\mathcal{B}_0}\Big(\rho_0\frac{u_i - 2u_i^0 + u_i^{00}}{\Delta t \Delta t}\delta u_i + J(\boldsymbol{F}^{-1})_{kj}\sigma_{ji}\frac{\partial \delta u_i}{\partial X_k} - \rho_0 f_i\delta u_i - J\mathcal{F}_i\delta u_i\Big)\,\mathrm{d}V + \sum_{\mathrm{outer}}\int_{\partial\mathcal{B}_0}\hat{t}_i\delta u_i\,\mathrm{d}A \tag{112}$$

Analogously, for computing the temperature we obtain the weak form by using the time discretization, applying the variational formulation, multiplying by Δt in order to bring it to the unit of energy, and integrating by parts

$$\begin{aligned}
\mathrm{F}_T = \int_{\mathcal{B}_0}\Big(\rho_0(\eta - \eta^0)\delta T - \Delta t\frac{Q_j}{T}\frac{\partial \delta T}{\partial X_j} - \Delta t\rho_0\frac{r}{T}\delta T + \Delta t\frac{Q_j}{T^2}\frac{\partial T}{\partial X_j}\delta T - \Delta t\frac{J}{T}\mathcal{E}_i\mathcal{J}_i^{\mathrm{fr.}}\delta T\Big)\,\mathrm{d}V + \\
+ \int_{\partial\mathcal{B}_0}\Delta t\frac{Q_j}{T}\delta T N_j \,\mathrm{d}A \ .
\end{aligned} \tag{113}$$

The assembly results in a jump term, which vanishes between the elements by means of Eqs. (59), $(64)_2$. On

the interface to the surrounding air, we model this jump as follows

$$\left[\!\left[Q_j N_j \right]\!\right] = h(T - T_{\text{ref.}}) \ , \tag{114}$$

with the convective heat transfer coefficient h furnishing an exchange between the continuum body and environment depending on the velocity of the surrounding fluid. This approximation is necessary since we skip to compute the velocity of the surrounding air directly. Analogously, on the computational boundary we set $T = T_{\text{ref.}}$ as DIRICHLET boundaries. The weak form to compute T in the LAGRANGEan frame reads

$$\begin{aligned} \mathrm{F}_T = \sum_{\text{ele.}} \int_{\mathcal{B}_0} \left(\rho_0(\eta - \eta^0)\delta T - \Delta t \frac{Q_j}{T} \frac{\partial \delta T}{\partial X_j} - \Delta t \rho_0 \frac{r}{T} \delta T + \Delta t \frac{Q_j}{T^2} \frac{\partial T}{\partial X_j} \delta T - \Delta t \frac{J}{T} \mathfrak{E}_i \mathfrak{j}_i^{\text{fr.}} \delta T \right) \mathrm{d}V + \\ + \sum_{\text{outer}} \int_{\partial \mathcal{B}_0} \Delta t \frac{h(T - T_{\text{ref.}})}{T} \delta T \, \mathrm{d}A \ . \end{aligned} \tag{115}$$

We recall that we solve for the same time instant $\mathrm{F}_\phi + \mathrm{F}_{\boldsymbol{A}}$ in the EULERian frame and $\mathrm{F}_{\boldsymbol{u}} + \mathrm{F}_T$ in the LAGRANGEan frame.

4.2. Mesh morphing

The weak form $\mathrm{F}_\phi + \mathrm{F}_{\boldsymbol{A}}$ in Eqs. (106) and (110) is solved in the EULERian frame for the whole computational domain, i.e., continuum body embedded in air (or vacuum). The whole computational domain includes the continuum body such that we need to move the continuum body to its current placement for solving the weak forms in the EULERian frame. The idea is similar to the fluid-structure interaction; however, the electromagnetic fields are also described within the continuum body. The weak form $\mathrm{F}_{\boldsymbol{u}} + \mathrm{F}_T$ in Eqs. (112), (115) needs to be solved in the LAGRANGEan frame only within the continuum body and not in the surrounding air. The motion of the continuum body within the computational domain connects these two frames such that we move the mesh by the displacement of the continuum body. This particular choice is justified by Eq. (56). For the surrounding air we spare solving the displacement such that we morph the surrounding domain in a particular way explained below in order to maintain the mesh quality.

A Delaunay triangulation is constructed from nodes in the moving material and on the fixed boundary using the positions in the original configuration. The nodes in the surrounding air are "glued" to this new triangle mesh. The displacement from the current configuration in the material is interpolated at air node position to give it a new position using the Barycentric coordinates of the node in the triangle as the shape functions for the interpolations. The connectivity of the original mesh is preserved during this process.

The Delaunay triangulation is computed using the Scipy module, which provides the Barycentric coordinate transform and fast point-in-triangle detection [65], [58]. The list of points of *fix_nodes* should contain a convex hull enclosing the domain, otherwise the interpolation is ill-defined.

4.3. Coupled time stepping algorithm

The thermomechanical fields $\boldsymbol{u}$ and T are defined on a submesh of the computational domain corresponding the material body. This submesh is defined as *matmesh* The electromagnetic potentials ϕ and $\boldsymbol{A}$ are defined on the mesh of the whole computational domain. They are coupled using a sequential time stepping scheme. At every time-step, the finite element coefficients from the electromagnetic finite element functions are mapped onto the equivalent coefficients on the submesh of the domain occupied by the continuum body. Then, the thermomechanical problem is solved for $\boldsymbol{u}$ and T at the next time-step. The displacement $\boldsymbol{u}$ is used to morph the mesh and then the thermomechanical fields are mapped onto the morphed mesh of the whole domain. The procedure of the time stepping algorithm is listed in Algorithm 2.

4.4. Implementation Details

The entire algorithm is implemented in Python using the open-source packages developed under the FEniCS project [47, 36, 48]. The mesh morphing algorithm, as well as other utility functions, is included for use in different applications in the library afqsfenicsutils.[3] The FEniCS implementation for the variational equations

[3]The git repository is located at `https://bitbucket.org/afqueiruga/afqsfenicsutil`

Algorithm 1 Calculate Mesh morphing procedure. Note, the variable *tris* is a list of tetrahedra in 3D.

Require: Nodes X, indices *fixed_nodes*
  $n_g \leftarrow$ Geometric dimension (2 or 3)
  $X_f \leftarrow X[\textit{fixed_nodes}]$
  $tris \leftarrow \text{Delaunay}(X_f)$
  Preallocate X'
  for $y \in X$ **and** $y \notin X_f$ **do**
    if $y \notin X_f$ **then**
      Find $t \in tris$ *s.t.* $y \in t$ using search tree.
      $B \leftarrow$ Barycentric transformation matrix of t
      $s[0 : n_g - 2] \leftarrow B \cdot y$
      $s[n-1] \leftarrow 1 - sum(s[0 : n_g - 2])$
      $y'[i] \leftarrow s[j] * X_f[t[j]][i]$ for $j = 0...n_g$ for $i = 0...n_g - 1$
      $X'[end] \leftarrow y'$
    else
      $X'[end] \leftarrow y$
    end if
  end for
  return X'

Algorithm 2 Main Simulation Procedure

  $mesh \leftarrow$ File
  $matmesh \leftarrow \subset mesh$ where $mesh$ is marked as material.
  $fix_nodes \leftarrow vertex_indices[matmesh \cup \partial mesh]$
  $u^{EM}, A^{EM} \leftarrow$ Thermomechanical and electromagnetic functions on $mesh$
  $u^{TM}, A^{TM} \leftarrow$ Thermomechanical and electromagnetic functions on $matmesh$
  while $t < t_{max}$ **do**
    Pull solution coefficients onto $matmesh$: $A^{TM}.coeffs[:] \leftarrow A^{EM}.coeffs[indices]$
    Solve $F^{TM}(u^{TM}; A^{TM}) = 0$ for $u^{TM}(t + \Delta t)$
    Push solution coefficients onto $mesh$: $u^{EM}.coeffs[indices] \leftarrow u^{TM}.coeffs[:]$
    $mesh.X \leftarrow \text{morph}(mesh.X + u^{EM}, fix_nodes)$
    Solve $F^{EM}(A^{EM}; u^{EM}) = 0$ for $A^{EM}(t + \Delta t)$
    $t \leftarrow t + \Delta t$
    Advance history: $A(t + \Delta t) \rightarrow A(t) \rightarrow A(t - \Delta t)$
  end while

and coupling system is available at the repository located at `https://github.com/afqueiruga/EMSI-2018`. (This repository will automatically download the independent libraries as a git submodule.) All codes are released under the GNU Public license as in [28].

5. Examples

We illustrate the functionality and versatility of the framework based upon the presented theoretical formulation and numerical algorithm by applying it to three engineering applications. We have chosen the examples where the interaction of thermomechanics with electromagnetism generates new design opportunities necessitating robust and accurate computation of such coupled and nonlinear multiphysics problem by using the simulation strategy developed herein.

Smart structure applications use materials with integrated sensor and actuator functionalities. There are only a few known natural materials presenting electromagnetic and mechanical coupling inherently. Therefore, functionalized materials are synthesized by combining materials with different abilities. In various branches of industry, these types of functionalized materials are applied in applications such health monitoring; shape, temperature, or vibration control; or energy harvesting. For examples by using a piezoelectric material, we refer to [92], [50], [69], [81], [41], [42], [44], [16], [93], [68], [88], [85], [66]. In [26], [24], [6], [12], [31], [46], [33], a magnetoelastic material is used for different applications. Thermoelectric coupling is demonstrated in [77], [96], [35]. We present three examples that are representative of new industry applications: a piezoelectric fan,

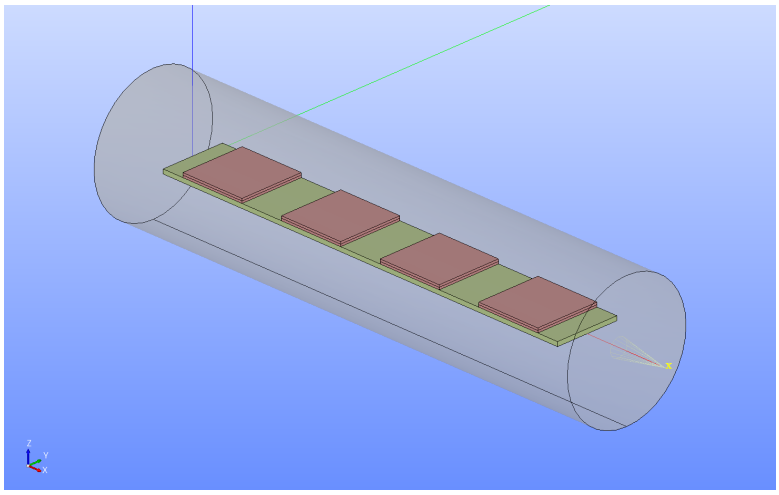

Figure 1: CAD model of the piezoelectric fan: on the epoxy beam (green), four piezoelectric patches (red) are attached comprising the continuum body $\mathcal{B}_0$ embedded in air (gray, transparent).

a magnetorheological elastomer, and a thermoelectric cooler.

5.1. Piezoelectric fan

A thin beam of 100 mm × 15 mm × 1 mm is modeled out of epoxy with four piezoelectric patches. Each patch is of two layers connected in parallel. In practice, many layers are used to increase the effect, herein we present a simplified computation with the geometry shown in Fig. 1. The continuum body, $\mathcal{B}_0$, is embedded in a cylindrical domain, modeling surrounding air, with far-away boundaries where the electromagnetic potentials vanish. Piezoelectric patches are made of 2 layers each of 0.5 mm thickness. They are poled along z-direction. For the piezoceramic and epoxy, we use the stiffness matrix C_{IJ} in Voigt's notation

$$C_{IJ} = \begin{pmatrix} C_{1111} & C_{1122} & C_{1133} & C_{1123} & C_{1113} & C_{1112} \\ C_{2211} & C_{2222} & C_{2233} & C_{2223} & C_{2213} & C_{2212} \\ C_{3311} & C_{3322} & C_{3333} & C_{3323} & C_{3313} & C_{3312} \\ C_{2311} & C_{2322} & C_{2333} & C_{2323} & C_{2313} & C_{2312} \\ C_{1311} & C_{1322} & C_{1333} & C_{1323} & C_{1313} & C_{1312} \\ C_{1211} & C_{1222} & C_{1233} & C_{1223} & C_{1213} & C_{1212} \end{pmatrix} . \tag{116}$$

Epoxy is an amorph material having translational and rotational symmetry such that the stiffness matrix is isotropic,

$$C_{IJ} = \begin{pmatrix} \lambda+2\mu & \lambda & \lambda & 0 & 0 & 0 \\ \lambda & \lambda+2\mu & \lambda & 0 & 0 & 0 \\ \lambda & \lambda & \lambda+2\mu & 0 & 0 & 0 \\ 0 & 0 & 0 & \mu & 0 & 0 \\ 0 & 0 & 0 & 0 & \mu & 0 \\ 0 & 0 & 0 & 0 & 0 & \mu \end{pmatrix} , \quad \lambda = \frac{(E-2G)G}{3G-E} , \quad \mu = G , \tag{117}$$

with Young's modulus E and shear modulus G. As piezoceramic we use PZT-5H poled along $z = x_3$. For this anisotropic PZT-5H, the compliance matrix

$$S_{IJ} = \begin{pmatrix} S_{11} & -\nu S_{11} & -\nu S_{11} & 0 & 0 & 0 \\ -\nu S_{11} & S_{11} & -\nu S_{11} & 0 & 0 & 0 \\ -\nu S_{11} & -\nu S_{11} & S_{33} & 0 & 0 & 0 \\ 0 & 0 & 0 & (1+\nu)S_{11} & 0 & 0 \\ 0 & 0 & 0 & 0 & (1+\nu)S_{11} & 0 \\ 0 & 0 & 0 & 0 & 0 & (1+\nu)S_{11} \end{pmatrix} , \tag{118}$$

is used to obtain the stiffness matrix $C_{IJ} = (S_{JI})^{-1}$. The piezoelectric constants, $\tilde{d}_{iJ}$, read

$$\tilde{d}_{iJ} = \begin{pmatrix} \tilde{d}_{111} & \tilde{d}_{122} & \tilde{d}_{133} & \tilde{d}_{123} & \tilde{d}_{131} & \tilde{d}_{112} \\ \tilde{d}_{211} & \tilde{d}_{222} & \tilde{d}_{233} & \tilde{d}_{223} & \tilde{d}_{231} & \tilde{d}_{212} \\ \tilde{d}_{311} & \tilde{d}_{322} & \tilde{d}_{333} & \tilde{d}_{323} & \tilde{d}_{331} & \tilde{d}_{312} \end{pmatrix} = \begin{pmatrix} 0 & 0 & 0 & 0 & \tilde{d}_{15} & 0 \\ 0 & 0 & 0 & \tilde{d}_{15} & 0 & 0 \\ \tilde{d}_{31} & \tilde{d}_{31} & \tilde{d}_{33} & 0 & 0 & 0 \end{pmatrix} , \tag{119}$$

where VOIGT's notation is applied on the last two indices (mapping to multiplication by the displacement gradient in VOIGT's notation). The susceptibility is given by the relative permittivity values by

$$\chi^{\text{el.}}_{ij} = \begin{pmatrix} \bar{\varepsilon}^{\text{el.}}_{11} & 0 & 0 \\ 0 & \bar{\varepsilon}^{\text{el.}}_{11} & 0 \\ 0 & 0 & \bar{\varepsilon}^{\text{el.}}_{33} \end{pmatrix} - \delta_{ij} \ . \tag{120}$$

We assume that the material has no piezomagnetic and magnetoelectric coupling, i.e., $\tilde{S}_{ijk} = 0$ and $\tilde{R}_{ij} = 0$, respectively. We compile all necessary material parameters in Table 3. Thermoelectric constant and electric conductivity is set to zero for the beam and patches. We apply a sinusoidal electric potential difference on the

Table 3: Material constants used in the simulation for the epoxy material, PZT-5H as the piezoceramic, and the surrounding air.

		Epoxy	PZT-5H	Air
Mass density	ρ in kg/m^3	2500	7500	
Compliance	S_{11} in m^2/N		$16.5 \cdot 10^{-12}$	
	S_{12} in m^2/N		$-4.78 \cdot 10^{-12}$	
	S_{13} in m^2/N		$-8.45 \cdot 10^{-12}$	
	S_{33} in m^2/N		$20.7 \cdot 10^{-12}$	
	S_{44} in m^2/N		$43.5 \cdot 10^{-12}$	
	S_{66} in m^2/N		$42.6 \cdot 10^{-12}$	
YOUNG's modulus	E in N/m^2	$30 \cdot 10^9$		
POISSON's ratio	ν	0.4		
Piezoelectric constants	$\tilde{d}_{33}$ in m/V	0	$585 \cdot 10^{-12}$	
	$\tilde{d}_{31}$ in m/V	0	$-265 \cdot 10^{-12}$	
	$\tilde{d}_{15}$ in m/V	0	$730 \cdot 10^{-12}$	
Dielectric constants	$\bar{\varepsilon}^{\text{el.}}_{33}$	1	3400	1
	$\bar{\varepsilon}^{\text{el.}}_{11}$	1	3130	1
Specific heat capacity	c in J/(kg K)	800	350	
Coefficients of thermal expansion	α_{33} in K^{-1}	$15 \cdot 10^{-6}$	$-4 \cdot 10^{-6}$	
	α_{11} in K^{-1}	$15 \cdot 10^{-6}$	$6 \cdot 10^{-6}$	
Thermal conductivity	κ in W/(m K)	1.3	1.1	

middle layer of 2 layers piezoelectric patch by grounding the bottom and upper faces. Along z-axis an electric field emerge that leads to a contraction along x as well as y-axis because of $\tilde{d}_{31}$. Since the potential difference from the middle to the top layer and from the middle to the bottom layer produces in electric fields that are opposed to each other in the each layer, one layer stretches when the other layer contracts. The bending in each patch bends the entire beam as shown in Fig. 2. We have applied a relatively big potential difference (amplitude) of 50 kV in order to generate a big deformation by using only 2 layers of patches. The displacement of the tip and the maximum temperature in the device over the course of the simulation is plotted in Fig. 3. Owing to the exaggerated potential difference, a significant temperature change occurs because of the electric field jump on the middle layer is generated as presented. Further engineering on this type of device would be needed to reduce the required potential difference and resultant heat production, which is possible due to the fully coupled simulation demonstrated.

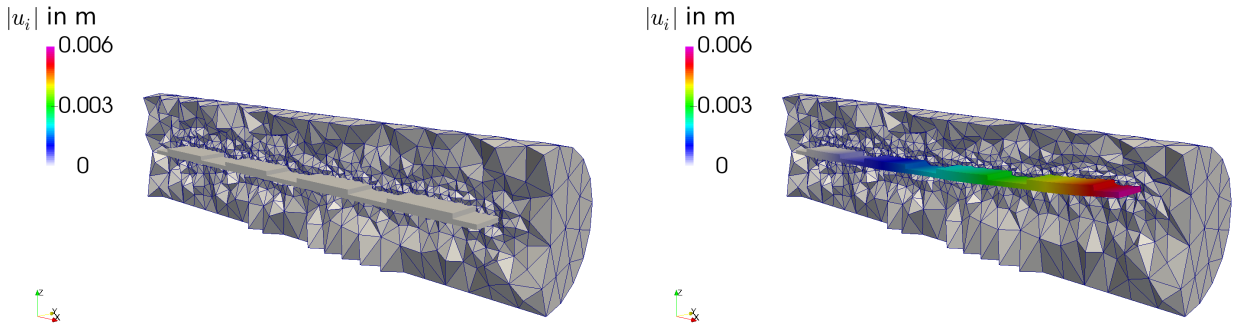

Figure 2: Configuration of the beam bend by the piezoelectric patches. The continuum body is colored by the magnitude of the displacement as well as morphed by the displacement *without* scaling. The air mesh is not colored by any field and has a crinkle cut to reveal the fan and illustrate the morphing of the elements.

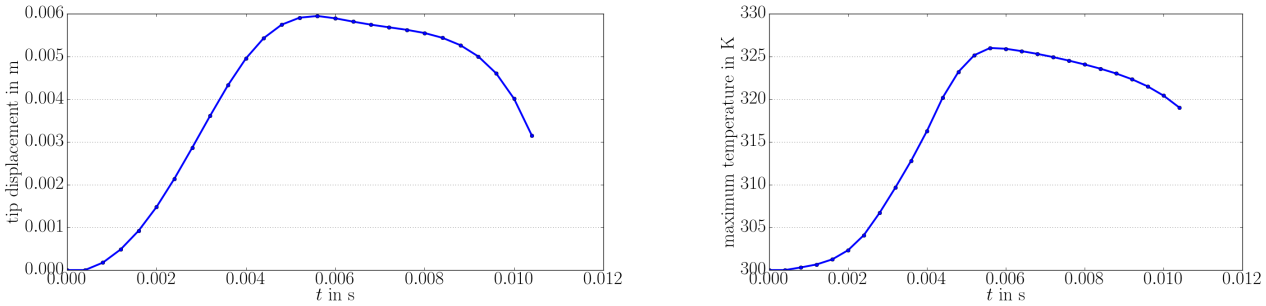

Figure 3: Displacement of the tip of the device (left) and the maximum temperature in the device (right) over the course of the simulation.

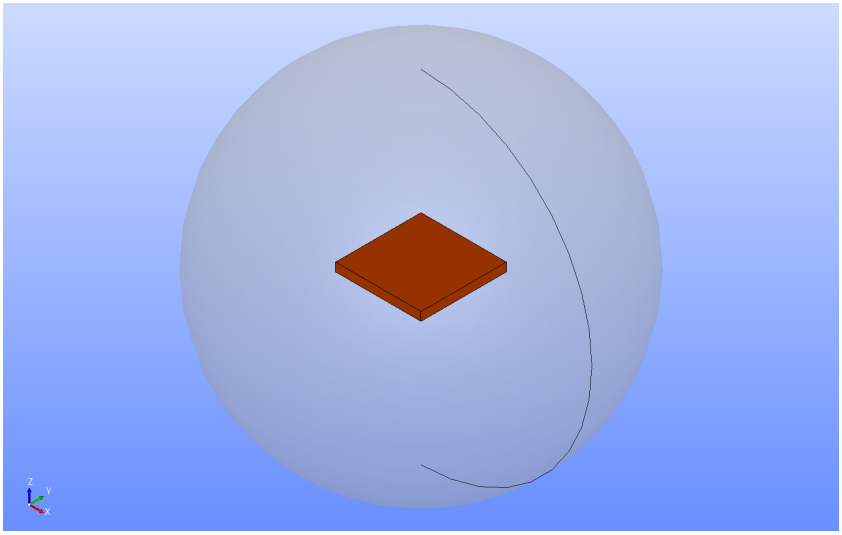

Figure 4: CAD model of the magnetorheological elastomer (orange) embedded in air (gray, transparent).

5.2. Magnetorheological elastomer

The deformation and magnetic field coupling is often called magnetostriction; but it is insignificant in natural materials. By designing a functionalized material, this behavior is used extensively for smart structures. Consider an elastomer filled with iron spherical particles with sizes on the order of micrometers. To model this material at the macroscopic scale, we homogenize the material into a magnetorheological elastomer. The thermomechanical behavior of the composite will be primarily representative of the elastomer matrix, with additional electromagnetic properties due to the iron additives. Because the iron particles are spherical, an elastomer with an amorph structure will remain isotropic if no external magnetic field was applied during the curing[46]. This crystalline structure with inversion symmetry prohibits any piezoelectric effects, $\tilde{T}_{ijk} = 0$. We assume that the magnetoelectric coupling vanishes, $\tilde{R}_{ij} = 0$. A piezoelectric effect is possible depending on the crosslinking of the polymer chains in the elastomer. A magnetoelectric coupling is also expected to arise as a consequence of this effect. The computational framework could include this effect with the necessary material constants, but it was neglected for this simulation.

The functionalized material considered is taken to be a silicone gel TSE2062 filled with carbonyl-iron particles. By assuming an equal and distinct distribution and successful curing, the elastomer has the thermomechanical properties of the silicon. This approximation depends on the relative amount of the iron particles used in the manufacturing. Increasing the amount leads to agglomerated particles building "bridges" between the distinct iron particles such that the thermomechanical characteristics of the composite material change dramatically. For an accurate treatment we refer to [98] and [97]. The material properties of the composite material—the particles embedded within the gel—are challenging to quantify, see the measurements in [37], [4], and [95]. Accurate material modeling of these measurements is also discussed heavily in the literature [15], [40], [78], [82], [57], [79], [55].

The following free energy density is the basis of the response:

$$\begin{aligned} \rho_0 f &= \frac{\mu}{4}\left(1+\tilde{\alpha}\tanh\left(\frac{I_4}{B_\mathrm{s}}\right)\right)\Big((1+n)(I_1-3)+(1-n)(I_2-3)\Big)+qI_4+rI_6\ , \\ C_{ij} &= F_{ji}F_{jk}\ ,\quad I_1 = C_{ii}\ ,\quad I_2 = \frac{1}{2}\Big(I_1^2 - C_{ij}C_{ji}\Big)\ ,\quad I_4 = B_iB_i\ ,\quad I_6 = C_{ij}B_jC_{ik}B_k\ . \end{aligned} \tag{121}$$

We have assumed an isochoric material as well as a neo-HOOKEan mechanical response. The parameters used for composite material are

$$\mu = 260\cdot 10^3\,\mathrm{Pa}\ ,\quad B_\mathrm{s} = 1\,\mathrm{T}^2\ ,\quad \tilde{\alpha} = 0.3\ ,\quad n = 0.3\ ,\quad q = r = \frac{1}{\mu_0}\ . \tag{122}$$

A simple plate of $10\,\mathrm{mm}\times 10\,\mathrm{mm}\times 1\,\mathrm{mm}$ is embedded in air as shown in Fig. 4. The plate is clamped on one side and a tangential traction is applied to opposite end oriented in the z-axis. We first apply the load with no

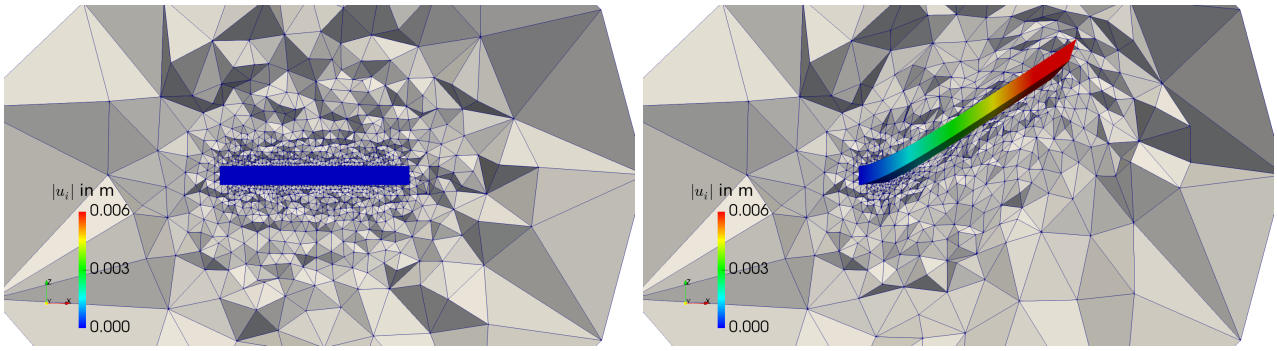

Figure 5: Configuration of the magnetorheological elastomer before and after the mechanical load is applied. The plate is colored by the magnitude of the displacement as well as morphed by the displacement *without* scaling. The air or vacuum mesh is not colored by any field and has a crinkle cut to present the morphing of the elements.

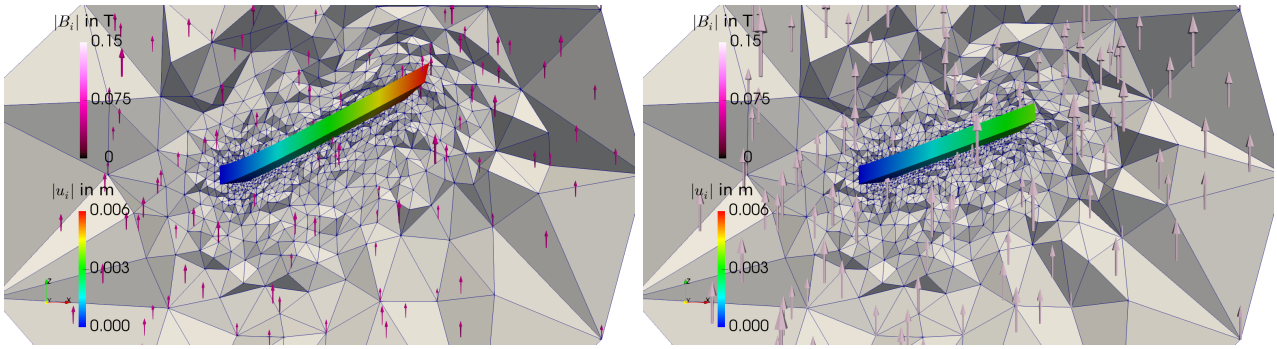

Figure 6: Configuration of the magnetorheological elastomer as the magnetic field is increased as 3 s (left) and 6 s (right). The arrows indicated the magnitude and orientation of the magnetic flux density B. The plate is colored by the magnitude of the displacement as well as morphed by the displacement *without* scaling. The air or vacuum mesh is not colored by any field and has a crinkle cut to present the morphing of the elements.

electromagnetic fields present, deforming it from its reference state into to an initial, deformed state shown in Fig. 5. This step is a performed as a nonlinear static solution of only the mechanical fields. We emphasize that no scaling is used such that the presented deformation is the actual computed deformation. The mechanical load is held constant throughout the rest of simulation. At the outer boundaries, $\partial\Omega$, the following magnetic potential is applied leading to a time-varying spatially-constant magnetic flux,

$$A_i = \begin{pmatrix} 0 \\ xB_\mathrm{o}\sin(2\pi\nu t) \\ 0 \end{pmatrix} \quad , \quad B_i = \epsilon_{ijk}\frac{\partial A_k}{\partial x_j} = \begin{pmatrix} 0 \\ 0 \\ B_\mathrm{o} \end{pmatrix} \quad , \quad \forall \boldsymbol{x} \in \partial\Omega \; . \tag{123}$$

The boundary conditions are $\phi = 0$ and the above form for A using a 10 s period, $\nu = 0.1$. The deformation change at 3 s and 6 s is presented in Fig. 6. As the magnetic field increases, the body effectively stiffens leading to a smaller deformation under the same applied force. The stiffening of the structure is controlled by the material parameters in Eq. (121), mainly by $\tilde{\alpha}$ until the saturation is achieved at B_s. As seen in Fig. 6, increasing B increases the stiffening effect, decreasing the magnitude of the deformation. This contactless stiffening mechanism could be used as either a sensor or actuator in a power transmission application where a winding (not included in the simulation) would be used to generate/sense the magnetic field.

5.3. Thermoelectric heat recovery

We demonstrate the applicability of the frame to typical component-based electronic devices by simulating a thermoelectric heat recovery strategy. The device is modeled as an assembly of two integrated circuits joined by copper traces, and a thermoelectric ceramic mounted on top of a substrate. The whole assembly is over molded in a silicon gel in order to reduce the environment effects such as corrosion (shown in the right side

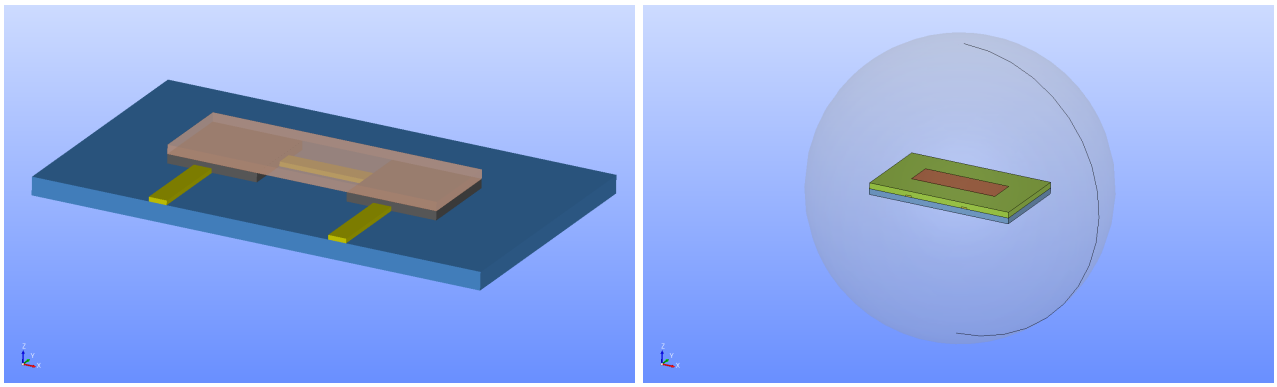

Figure 7: A simplified circuit board. Left: On the board (blue) two microchips (gray) are attached that are connected by traces (yellow). On top of the chips a thermoelectric ceramic (transparent, orange) is placed. Right: The whole assembly out of the board, chips, traces overmolded by a silicon gel (green) is embedded in air (transparent, gray).

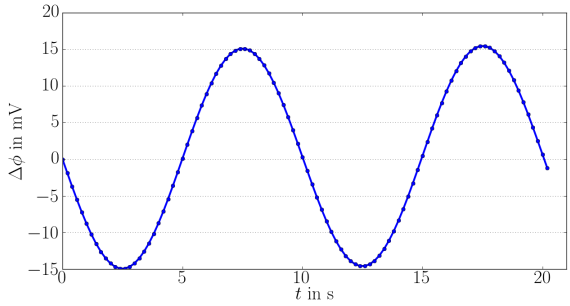

Figure 8: Output of the thermoelectric device, electric potential difference, $\Delta\phi$ in mV, as a result of AC put over the traces.

of Fig 7. Because of the environmental large temperature changes, thermal stresses appear and the chosen gel affects the reliability of the assembly as well. An alternating current (AC) is used with an electric potential difference of 12 V on the trace endings in front as seen in Fig. 7. During operation of the device, Joule heating causes a temperature change that effects energy recovery through the thermoelectric material. This produces an increase in the temperature leading to an electric current across the piezoceramic sheet measured as a potential difference. This sheet includes an assembly of conductive materials with a thermoelectric constant π generating an electric current in Eq. (93) because of a temperature difference. The simplified geometry is shown in Fig. 7. The board is out of a composite material, mostly glass reinforced epoxy resin. The microchips are represented as ceramic materials without the detailed internal assembly. As an electric current passes the chip, due to the resistance, it heats up. Communication traces between the two integrated circuits are simplified to a sole copper element (instead of discretizing each of the dozens independent traces that would normally be present.)

The endpoints at the traces in frontside of the device (apparent on the left side of Fig. 7, a given electric potential difference creates an electric current through the chips leading to Joule's heating. A temperature difference causes a heat flux and in addition to that an electric current. The chips heat up the thermoelectric ceramic sheet from below, at the same time, on top of the sheet a cooling agent (like water in a closed system) reduces the temperature by a mixed boundary condition, $h(T-T_{\text{ref.}})$, with a high convection constant $h = 10^5\,\text{J}/(\text{s}\,\text{m}^2\,\text{K})$.

We record this difference over time and present in Fig. 8. The thermoelectric energy harvesting shown in this simulation is not effective enough for this type of device. However, it can be used in clusters or in environments, where receiving energy is challenging. It is important to notice that this coupling is inherent in the material and no degradation is expected to occur.

6. Conclusion

We have developed a complete theory of continuum mechanics with electromagnetic interaction in solid bodies under large deformations. Balance equations for mechanical, thermal, and electromagnetic fields have been discussed and all necessary constitutive equations have been derived by exploiting thermodynamical principles. The constitutive equations are the simplest possible, where linear relations are used neglecting viscous response and electromagnetic hysteresis have been ignored. Despite the linearized form of the responses, the resulting variational form is nonlinear with complete coupling of all of the mechanical and electromagnetic fields. In order to reduce the computational cost, we have proposed a novel method and solve electromagnetic fields in the whole domain, whereas the deformation and temperature are solved only within the continuum body. Separation of field and matter is possible; however, their equations are defined in different placements. Therefore, from the very beginning of the development of the theory, we have emphasized different placements by using an explicit notation. Numerical solution in two different placements is possible by using a staggered time integration scheme as the mesh morphing algorithm presented. The nonlinear variational forms were implemented using the finite element method using FEniCS. In order to encourage further achievements, the mesh morphing algorithm implementation is released under the GNU LGPL `https://github.com/afqueiruga/afqsfenicsutil` and the scripts and geometry files that performed the simulations are released under the GNU GPL at the repository `https://github.com/afqueiruga/EMSI-2018`.

References

[1] B. E. Abali.
Computational Reality, Solving Nonlinear and Coupled Problems in Continuum Mechanics.
Advanced Structured Materials. Springer, 2016.
ISBN 978-981-10-2443-6.

[2] B. E. Abali and F. A. Reich.
Thermodynamically consistent derivation and computation of electro-thermo-mechanical systems for solid bodies.
Computer Methods in Applied Mechanics and Engineering, 2017.

[3] Sheikh N Ahmad, CS Upadhyay, and C Venkatesan.
Electro-thermo-elastic formulation for the analysis of smart structures.
Smart materials and structures, 15(2):401, 2006.

[4] Haining An, Stephen J Picken, and Eduardo Mendes.
Nonlinear rheological study of magneto responsive soft gels.
Polymer, 53(19):4164–4170, 2012.

[5] Douglas N Arnold and Anders Logg.
Periodic table of the finite elements.
SIAM News, 47(9), 2014.

[6] G Ausanio, AC Barone, C Hison, V Iannotti, G Mannara, and L Lanotte.
Magnetoelastic sensor application in civil buildings monitoring.
Sensors and Actuators A: Physical, 123:290–295, 2005.

[7] Matthew I Barham, Daniel A White, and David J Steigmann.
Finite element modeling of the deformation of magnetoelastic film.
Journal of Computational Physics, 229(18):6193–6207, 2010.

[8] Stephen M Barnett.
Resolution of the Abraham–Minkowski dilemma.
Physical Review Letters, 104(7):070401, 2010.

[9] Sascha Baumanns, Markus Clemens, and Sebastian Schops.
Structural aspects of regularized full maxwell electrodynamic potential formulations using fit.
In *Electromagnetic Theory (EMTS), Proceedings of 2013 URSI International Symposium on*, pages 1007–1010. IEEE, 2013.

[10] A Benjeddou.
Advances in piezoelectric finite element modeling of adaptive structural elements: a survey.
Computers & Structures, 76(1):347–363, 2000.

[11] Max Bethune-Waddell and Kenneth J Chau.
Simulations of radiation pressure experiments narrow down the energy and momentum of light in matter.
Reports on Progress in Physics, 78(12):122401, 2015.

[12] A Bieńkowski, R Szewczyk, and J Salach.
Industrial application of magnetoelastic force and torque sensors.
Acta Physica Polonica A, 118(5):1008–1009, 2010.

[13] Alain Bossavit.
Whitney forms: A class of finite elements for three-dimensional computations in electromagnetism.
IEE Proceedings A (Physical Science, Measurement and Instrumentation, Management and Education, Reviews), 135(8):493–500, 1988.

[14] Sylvain D Brechet and Jean-Philippe Ansermet.
Thermodynamics of continuous media with intrinsic rotation and magnetoelectric coupling.
Continuum Mechanics and Thermodynamics, 26(2):115–142, 2014.

[15] IA Brigadnov and A Dorfmann.
Mathematical modeling of magneto-sensitive elastomers.
International Journal of Solids and Structures, 40(18):4659–4674, 2003.

[16] Andreas J Brunner, Marcel Birchmeier, Mark M Melnykowycz, and Michel Barbezat.
Piezoelectric fiber composites as sensor elements for structural health monitoring and adaptive material systems.
Journal of Intelligent Material Systems and Structures, 20(9):1045–1055, 2009.

[17] Robert C Cammarata.
Surface and interface stress effects in thin films.
Progress in surface science, 46(1):1–38, 1994.

[18] C. Caratheodory.
Untersuchungen über die Grundlagen der Thermodynamik.
Mathematische Annalen, 67(3):355–386, 1909.
URL `http://dx.doi.org/10.1007/BF01450409`.

[19] Lan Jen Chu, Hermann A Haus, and P Penfield Jr.
The force density in polarizable and magnetizable fluids.
Proceedings of the IEEE, 54(7):920–935, 1966.

[20] Patrick Ciarlet Jr and Jun Zou.
Fully discrete finite element approaches for time-dependent maxwell's equations.
Numerische Mathematik, 82(2):193–219, 1999.

[21] Leszek Demkowicz.
Computing with hp-adaptive finite elements: volume 1 one and two dimensional elliptic and Maxwell problems.
CRC Press, 2006.

[22] JL Ericksen.
On formulating and assessing continuum theories of electromagnetic fields in elastic materials.
Journal of Elasticity, 87(2-3):95–108, 2007.

[23] A Cemal Eringen and Gérard A Maugin.
Electrodynamics of Continua I: Foundations and Solid Media.
Springer, 1990.

[24] M Frommberger, Ch Zanke, A Ludwig, M Tewes, and E Quandt.
Processing and application of magnetoelastic thin films in high-frequency devices.
Microelectronic engineering, 67:588–594, 2003.

[25] Andrew Gillette, Alexander Rand, and Chandrajit Bajaj.
Construction of scalar and vector finite element families on polygonal and polyhedral meshes.
Computational Methods in Applied Mathematics, 16(4):667–683, 2016.

[26] John M Ginder, Mark E Nichols, Larry D Elie, and Janice L Tardiff.
Magnetorheological elastomers: properties and applications.
In *Smart Structures and Materials 1999: Smart Materials Technologies*, volume 3675, pages 131–139. International Society for Optics and Photonics, 1999.

[27] Sebastian Glane, Felix A Reich, and Wolfgang H Müller.
Modeling of non-ideal hard permanent magnets with an affine-linear model, illustrated for a bar and a horseshoe magnet.
Continuum Mechanics and Thermodynamics, pages 1–21, 2017.

[28] GNU Public.
Gnu general public license.
http://www.gnu.org/copyleft/gpl.html, June 2007.

[29] David J Griffiths.
Resource letter em-1: Electromagnetic momentum.
American Journal of Physics, 80(1):7–18, 2012.

[30] David Jeffrey Griffiths and Reed College.
Introduction to electrodynamics, volume 3.
prentice Hall Upper Saddle River, NJ, 1999.

[31] Craig A Grimes, Somnath C Roy, Sanju Rani, and Qingyun Cai.
Theory, instrumentation and applications of magnetoelastic resonance sensors: a review.
Sensors, 11(3):2809–2844, 2011.

[32] S.R. Groot and P. Mazur.
Non-equilibrium thermodynamics, 1984.

[33] Xing Guo, Shengbo Sang, Jinyu Guo, Aoqun Jian, Qianqian Duan, Jianlong Ji, Qiang Zhang, and Wendong Zhang.
A magnetoelastic biosensor based on e2 glycoprotein for wireless detection of classical swine fever virus e2 antibody.
Scientific reports, 7(1):15626, 2017.

[34] O. R. Hachkevych and R. F. Terlets'kyi.
Models of thermomechanics of magnetizable and polarizable conducting deformable solids.
Materials Science, 40(3):320–336, 2004.

[35] Wei He, Gan Zhang, Xingxing Zhang, Jie Ji, Guiqiang Li, and Xudong Zhao.
Recent development and application of thermoelectric generator and cooler.
Applied Energy, 143:1–25, 2015.

[36] J. Hoffman, J. Jansson, C. Johnson, M. Knepley, RC Kirby, A. Logg, L. R. Scott, and G. N. Wells.
FEniCS.
http://www.fenicsproject.org/, 2005.

[37] Mark R Jolly, J David Carlson, Beth C Muñoz, and Todd A Bullions.
The magnetoviscoelastic response of elastomer composites consisting of ferrous particles embedded in a polymer matrix.
Journal of Intelligent Material Systems and Structures, 7(6):613–622, 1996.

[38] D. S. Jones.
The Theory of Electromagnetism.
Pergamon, 1964.
ISBN 978-0-08-013686-8.
doi: http://dx.doi.org/10.1016/B978-0-08-013686-8.50006-X.
URL `http://www.sciencedirect.com/science/article/pii/B978008013686850006X`.

[39] David Jou, Jose Casas-Vazquez, and Georgy Lebon.
Extended irreversible thermodynamics revisited (1988-98).
Reports on Progress in Physics, 62(7):1035, 1999.

[40] SV Kankanala and N Triantafyllidis.
On finitely strained magnetorheological elastomers.
Journal of the Mechanics and Physics of Solids, 52(12):2869–2908, 2004.

[41] Dae-Kwan Kim and Jae-Hung Han.
Smart flapping wing using macrofiber composite actuators.
In *Smart Structures and Materials*, pages 61730F–61730F. International Society for Optics and Photonics, 2006.

[42] A Kovalovs, E Barkanov, and S Gluhihs.
Active control of structures using macro-fiber composite (mfc).
In *Journal of Physics: Conference Series*, volume 93, page 012034. IOP Publishing, 2007.

[43] Attay Kovetz.
Electromagnetic theory.
2000.

[44] Francesco Lanza Discalea, Howard Matt, Ivan Bartoli, Stefano Coccia, Gyuhae Park, and Charles Farrar.
Health monitoring of uav wing skin-to-spar joints using guided waves and macro fiber composite transducers.
Journal of intelligent material systems and structures, 18(4):373–388, 2007.

[45] Jichun Li.
Numerical convergence and physical fidelity analysis for Maxwell's equations in metamaterials.
Computer Methods in Applied Mechanics and Engineering, 198(37):3161–3172, 2009.

[46] WH Li, XZ Zhang, and H Du.
Magnetorheological elastomers and their applications.
In *Advances in Elastomers I*, pages 357–374. Springer, 2013.

[47] A. Logg and G. N. Wells.
Dolfin: Automated finite element computing.
ACM Transactions on Mathematical Software, 37(2), 2010.
URL `http://www.dspace.cam.ac.uk/handle/1810/221918/`.

[48] A. Logg, K. A. Mardal, and G. N. Wells.
Automated Solution of Differential Equations by the Finite Element Method, The FEniCS Book, volume 84 of *Lecture Notes in Computational Science and Engineering.*
Springer, 2011.

[49] HA Lorentz.
Zittungsverlagen akad. van wettenschappen 1, 74 (nov. 26, 1892); versuch einer theorie der elektrischen und optischen erscheinungen in bewegten körpern, brill, leiden, 1895.
Proc. Acad. Sci.(Amsterdam)(Engl. version), 6:809, 1904.

[50] Armand Losinski.
Low-profile axial-flow single-blade piezoelectric fan, January 19 1999.
US Patent 5,861,703.

[51] Francis E Low.
Classical field theory: electromagnetism and gravitation.
Wiley-VCH Verlag, 2004.

[52] Masud Mansuripur.
Resolution of the abraham–minkowski controversy.
Optics Communications, 283(10):1997–2005, 2010.

[53] James Clerk Maxwell.
A Treatise on Electricity and Magnetism.
Oxford at the Clarendon Press, 1892.

[54] CW Mays, JS Vermaak, and D Kuhlmann-Wilsdorf.
On surface stress and surface tension: Ii. determination of the surface stress of gold.
Surface science, 12(2):134–140, 1968.

[55] Markus Mehnert, Mokarram Hossain, and Paul Steinmann.
Towards a thermo-magneto-mechanical coupling framework for magneto-rheological elastomers.
International Journal of Solids and Structures, 2017.

[56] A Meitzler, HF Tiersten, AW Warner, D Berlincourt, GA Couqin, and FS Welsh III.
Ieee standard on piezoelectricity, 1988.

[57] Philipp Metsch, Karl A Kalina, Christian Spieler, and Markus Kästner.
A numerical study on magnetostrictive phenomena in magnetorheological elastomers.
Computational Materials Science, 124:364–374, 2016.

[58] K Jarrod Millman and Michael Aivazis.
Python for scientists and engineers.
Computing in Science & Engineering, 13(2):9–12, 2011.

[59] Wolfgang H. Mueller and Muschik W.
Bilanzgleichungen offener mehrkomponentiger Systeme I. Massen- und Impulsbilanzen.
J. Non-Equilib. Thermodyn., 8:29–46, 1983.

[60] I. Müller.
Thermodynamics.
Pitman Publishing, London, 1985.

[61] Ingo Müller and Tommaso Ruggeri.
Rational extended thermodynamics, volume 37.
Springer Science & Business Media, 2013.

[62] Muschik W. and Wolfgang H. Mueller.
Bilanzgleichungen offener mehrkomponentiger Systeme II. Energie- und Entropiebilanz.
J. Non-Equilib. Thermodyn., 8:47–66, 1983.

[63] Jean-Claude Nédélec.
Mixed finite elements in R3.
Numerische Mathematik, 35(3):315–341, 1980.

[64] Yuri N Obukhov.
Electromagnetic energy and momentum in moving media.
Annalen der Physik, 17(9-10):830–851, 2008.

[65] Travis E Oliphant.
Python for scientific computing.
Computing in Science & Engineering, 9(3), 2007.

[66] Kenny Pagel, Welf-Guntram Drossel, and Wolfgang Zorn.
Multi-functional shape-memory-actuator with guidance function.
Production Engineering, 7(5):491–496, 2013.

[67] Yih-Hsing Pao and Kolumban Hutter.
Electrodynamics for moving elastic solids and viscous fluids.
Proceedings of the IEEE, 63(7):1011–1021, 1975.

[68] Rolf Paradies and Paolo Ciresa.
Active wing design with integrated flight control using piezoelectric macro fiber composites.
Smart Materials and Structures, 18(3):035010, 2009.

[69] Gyuhae Park, Hoon Sohn, Charles R Farrar, and Daniel J Inman.
Overview of piezoelectric impedance-based health monitoring and path forward.
Shock and Vibration Digest, 35(6):451–463, 2003.

[70] W. Pauli.
Thermodynamics and the Kinetic Theory of Gases: Volume 3 of Pauli Lectures on Physics, volume 3.
Dover Publications (2010) repub. of MIT Press, 1973.

[71] Jean-Paul Pelteret, Denis Davydov, Andrew McBride, Duc Khoi Vu, and Paul Steinmann.
Computational electro-elasticity and magneto-elasticity for quasi-incompressible media immersed in free space.
International Journal for Numerical Methods in Engineering, 108(11):1307–1342, 2016.

[72] Alejandro Queiruga and Tarek Zohdi.
Microscale modeling of effective mechanical and electrical properties of textiles.
International Journal for Numerical Methods in Engineering, 108(13):1603–1625, 2016.

[73] Alejandro Francisco Queiruga and Tarek I Zohdi.
Formulation and numerical analysis of a fully-coupled dynamically deforming electromagnetic wire.
Computer Methods in Applied Mechanics and Engineering, 305:292–315, 2016.

[74] Pierre-Arnaud Raviart and Jean-Marie Thomas.
A mixed finite element method for 2-nd order elliptic problems.
In *Mathematical aspects of finite element methods*, pages 292–315. Springer, 1977.

[75] Robert N Rieben, Daniel A White, Brad K Wallin, and JM Solberg.
An arbitrary lagrangian–eulerian discretization of mhd on 3d unstructured grids.
Journal of Computational Physics, 226(1):534–570, 2007.

[76] Phoebus Rosakis.
Ellipticity and deformations with discontinuous gradients in finite elastostatics.
Archive for Rational Mechanics and Analysis, 109(1):1–37, 1990.

[77] Ioan Sauciuc and Gregory M Chrysler.
Electronic thermal management, April 18 2006.
US Patent 7,031,155.

[78] Prashant Saxena, Mokarram Hossain, and Paul Steinmann.
Nonlinear magneto-viscoelasticity of transversally isotropic magneto-active polymers.
In *Proc. R. Soc. A*, volume 470, page 20140082. The Royal Society, 2014.

[79] Gerlind Schubert and Philip Harrison.
Magnetic induction measurements and identification of the permeability of magneto-rheological elastomers using finite element simulations.
Journal of Magnetism and Magnetic Materials, 404:205–214, 2016.

[80] Ro Shuttleworth.
The surface tension of solids.
Proceedings of the Physical Society. Section A, 63(5):444, 1950.

[81] Henry A Sodano, Daniel J Inman, and Gyuhae Park.
Comparison of piezoelectric energy harvesting devices for recharging batteries.
Journal of Intelligent Material Systems and Structures, 16(10):799–807, 2005.

[82] C Spieler, P Metsch, M Kästner, and V Ulbricht.
Microscale modeling of magnetoactive composites undergoing large deformations.
Technische Mechanik, 34(1):39–50, 2014.

[83] M Stiemer, J Unger, B Svendsen, and H Blum.
An arbitrary lagrangian eulerian approach to the three-dimensional simulation of electromagnetic forming.
Computer Methods in Applied Mechanics and Engineering, 198(17):1535–1547, 2009.

[84] B Svendsen and T Chanda.
Continuum thermodynamic formulation of models for electromagnetic thermoinelastic solids with application in electromagnetic metal forming.
Continuum Mechanics and Thermodynamics, 17(1):1–16, 2005.

[85] Masayoshi Tanida, Midori Sunaga, and Hiroaki Wada.
Piezoelectric fan and air cooling apparatus using the piezoelectric fan, February 14 2013.
US Patent App. 13/370,341.

[86] Leslie Ronald George Treloar.
The physics of rubber elasticity.
Oxford University Press, USA, 1975.

[87] C. Truesdell and R. A. Toupin.
Encyclopedia of physics, volume III/1, principles of classical mechanics and field theory, chapter The classical field theories, pages 226–790.
Springer-Verlag, Berlin/Göttingen/Heidelberg, 1960.

[88] Jan-Willem Van Wingerden, Anton Hulskamp, Thanasis Barlas, Ivo Houtzager, Harald Bersee, Gijs van Kuik, and Michel Verhaegen.
Two-degree-of-freedom active vibration control of a prototyped "smart" rotor.
IEEE transactions on control systems technology, 19(2):284–296, 2011.

[89] JS Vermaak, CW Mays, and D Kuhlmann-Wilsdorf.
On surface stress and surface tension: I. theoretical considerations.
Surface Science, 12(2):128–133, 1968.

[90] Philippe Vidal, Michele D'Ottavio, Mehdi Ben Thaïer, and Olivier Polit.
An efficient finite shell element for the static response of piezoelectric laminates.
Journal of Intelligent Material Systems and Structures, 22(7):671–690, 2011.

[91] Franziska Vogel, Roger Bustamante, and Paul Steinmann.
On some mixed variational principles in magneto-elastostatics.
International Journal of Non-Linear Mechanics, 51:157–169, 2013.

[92] Yasuo Yamada, Katsumi Fujimoto, and Jiro Inoue.
Piezoelectric fan, October 25 1988.
US Patent 4,780,062.

[93] Yaowen Yang, Lihua Tang, and Hongyun Li.
Vibration energy harvesting using macro-fiber composites.
Smart materials and structures, 18(11):115025, 2009.

[94] Sung Yi, Shih Fu Ling, Ming Ying, Harry H Hilton, and Jack R Vinson.
Finite element formulation for anisotropic coupled piezoelectro-hygro-thermo-viscoelasto-dynamic problems.
International journal for numerical methods in engineering, 45(11):1531–1546, 1999.

[95] Miao Yu, Song Qi, Jie Fu, Mi Zhu, and Dong Chen.
Understanding the reinforcing behaviors of polyaniline-modified carbonyl iron particles in magnetorheological elastomer based on polyurethane/epoxy resin ipns matrix.
Composites Science and Technology, 139:36–46, 2017.

[96] Dongliang Zhao and Gang Tan.
A review of thermoelectric cooling: materials, modeling and applications.
Applied Thermal Engineering, 66(1):15–24, 2014.

[97] Tarek I Zohdi.
Electromagnetic properties of multiphase dielectrics: a primer on modeling, theory and computation, volume 64.
Springer Science & Business Media, 2012.

[98] Tarek I Zohdi and Peter Wriggers.
An introduction to computational micromechanics.
Springer Science & Business Media, 2008.

A. Electric current due to the bound charges

By using

$$D_i = \mathfrak{D}_i - P_i \ , \quad H_i = \mathfrak{H}_i + \mathcal{M}_i \tag{124}$$

in Maxwell's equations

$$\begin{aligned} \frac{\partial \mathfrak{D}_i}{\partial x_i} - \frac{\partial P_i}{\partial x_i} &= \rho z^{\text{fr.}} + \rho z^{\text{bo.}} \ , \\ -\frac{\partial \mathfrak{D}_i}{\partial t} + \frac{\partial P_i}{\partial t} + \epsilon_{ijk}\frac{\partial \mathfrak{H}_k}{\partial x_j} + \epsilon_{ijk}\frac{\partial \mathcal{M}_k}{\partial x_j} &= J_i \ , \end{aligned} \tag{125}$$

we realize

$$\begin{aligned} \frac{\partial \mathfrak{D}_i}{\partial x_i} = \rho z^{\text{fr.}} \ , \quad -\frac{\partial P_i}{\partial x_i} &= \rho z^{\text{bo.}} \ , \\ -\frac{\partial \mathfrak{D}_i}{\partial t} + \epsilon_{ijk}\frac{\partial \mathfrak{H}_k}{\partial x_j} = J_i - \frac{\partial P_i}{\partial t} - \epsilon_{ijk}\frac{\partial \mathcal{M}_k}{\partial x_j} &= J_i^{\text{fr.}} \ . \end{aligned} \tag{126}$$

B. Balance of electromagnetic momentum

We start by obtaining the time rate of the chosen electromagnetic momentum

$$\frac{\partial \mathcal{G}_i}{\partial t} = \frac{\partial \epsilon_{ijk}\mathfrak{D}_j B_k}{\partial t} = \epsilon_{ijk}\frac{\partial D_j B_k}{\partial t} + \epsilon_{ijk}\frac{\partial P_j B_k}{\partial t} \ . \tag{127}$$

The first term can be rewritten, by using

$$\epsilon_{ijk} = -\epsilon_{ikj} \ , \quad \epsilon_{ijk}\epsilon_{klm} = \delta_{il}\delta_{jm} - \delta_{im}\delta_{jl} \ , \tag{128}$$

as well as Maxwell's equations

$$\begin{aligned} \epsilon_{ijk}\frac{\partial D_j B_k}{\partial t} &= \epsilon_{ijk}\Big(\epsilon_{jlm}\frac{\partial H_m}{\partial x_l} - J_j\Big)B_k - \epsilon_{ijk}D_j\epsilon_{klm}\frac{\partial E_m}{\partial x_l} = \\ &= -\frac{\partial H_k}{\partial x_i}B_k + \frac{\partial H_i}{\partial x_k}B_k - (\boldsymbol{J}\times\boldsymbol{B})_i - D_j\frac{\partial E_j}{\partial x_i} + D_j\frac{\partial E_i}{\partial x_j} \ . \end{aligned} \tag{129}$$

Moreover, by using Maxwell–Lorentz aether relations we observe

$$\begin{aligned} \frac{\partial H_k}{\partial x_i}B_k = \frac{1}{\mu_0}\frac{\partial B_k}{\partial x_i}B_k = \frac{1}{\mu_0}\frac{\partial}{\partial x_i}\Big(\frac{1}{2}B_k B_k\Big) = \frac{1}{2}\frac{\partial H_k B_k}{\partial x_i} \ , \\ D_j\frac{\partial E_j}{\partial x_i} = \varepsilon_0 E_j\frac{\partial E_j}{\partial x_i} = \varepsilon_0\frac{\partial}{\partial x_i}\Big(\frac{1}{2}E_j E_j\Big) = \frac{1}{2}\frac{\partial D_j E_j}{\partial x_i} \ . \end{aligned} \tag{130}$$

Finally, by utilizing Maxwell's equations we achieve

$$\begin{aligned} \frac{\partial H_i}{\partial x_k}B_k = \frac{\partial H_i B_k}{\partial x_k} \ , \\ D_j\frac{\partial E_i}{\partial x_j} = \frac{\partial D_j E_i}{\partial x_j} - \rho z E_i \ . \end{aligned} \tag{131}$$

By combining all above, we obtain

$$\frac{\partial \mathcal{G}_i}{\partial t} = \frac{\partial}{\partial x_j}\underbrace{\Big(-\frac{1}{2}\delta_{ij}\big(D_k E_k + H_k B_k\big) + H_i B_j + D_j E_i\Big)}_{m_{ji}} - \underbrace{\Big(\rho z E_i + (\boldsymbol{J}\times\boldsymbol{B})_i - \frac{\partial(\boldsymbol{P}\times\boldsymbol{B})_i}{\partial t}\Big)}_{\mathcal{F}_i} \ , \tag{132}$$

after comparing to the the balance of electromagnetic momentum.

C. Balance of electromagnetic energy

By starting with the divergence of the chosen electromagnetic flux

$$\frac{\partial \mathcal{P}_i}{\partial x_i} = \epsilon_{ijk}\frac{\partial \mathfrak{H}_j E_k}{\partial x_i} = \epsilon_{ijk}\frac{\partial H_j E_k}{\partial x_i} - \underbrace{\epsilon_{ijk}\frac{\partial \mathcal{M}_j E_k}{\partial x_i}}_{\frac{\partial (\boldsymbol{\mathcal{M}}\times\boldsymbol{E})_i}{\partial x_i}} \ , \tag{133}$$

we can rewrite the first term by using $\epsilon_{ijk} = \epsilon_{jki} = \epsilon_{kij}$ and $\epsilon_{ijk} = -\epsilon_{jik}$, as well as inserting MAXWELL's equations,

$$\begin{aligned}\epsilon_{ijk}\frac{\partial H_j E_k}{\partial x_i} = \epsilon_{kij}\frac{\partial H_j}{\partial x_i}E_k - H_j\epsilon_{jik}\frac{\partial E_k}{\partial x_i} = \Big(\frac{\partial D_k}{\partial t} + J_k\Big)E_k + H_j\frac{\partial B_j}{\partial t} = \\ = \frac{\partial}{\partial t}\Big(\frac{1}{2}D_k E_k + \frac{1}{2}H_j B_j\Big) + J_k E_k \ .\end{aligned} \tag{134}$$

Since we have

$$\begin{aligned}J_i E_i = \Big(J_i^{\text{fr.}} + \frac{\partial P_i}{\partial t} + \epsilon_{ijk}\frac{\partial \mathcal{M}_k}{\partial x_j}\Big)E_i = J_i^{\text{fr.}}E_i + \frac{\partial P_i E_i}{\partial t} - P_i\frac{\partial E_i}{\partial t} + \epsilon_{ijk}\frac{\partial \mathcal{M}_k E_i}{\partial x_j} - \mathcal{M}_k\epsilon_{ijk}\frac{\partial E_i}{\partial x_j} = \\ = J_i^{\text{fr.}}E_i + \frac{\partial P_i E_i}{\partial t} - P_i\frac{\partial E_i}{\partial t} + \epsilon_{jki}\frac{\partial \mathcal{M}_k E_i}{\partial x_j} + \mathcal{M}_k\epsilon_{kji}\frac{\partial E_i}{\partial x_j} = J_i^{\text{fr.}}E_i + \frac{\partial P_i E_i}{\partial t} - P_i\frac{\partial E_i}{\partial t} + \frac{\partial (\boldsymbol{\mathcal{M}}\times\boldsymbol{E})_j}{\partial x_j} - \mathcal{M}_k\frac{\partial B_k}{\partial t} = \\ = J_i^{\text{fr.}}E_i + \frac{\partial}{\partial t}(P_i E_i - \mathcal{M}_i B_i) - P_i\frac{\partial E_i}{\partial t} + \frac{\partial (\boldsymbol{\mathcal{M}}\times\boldsymbol{E})_j}{\partial x_j} + B_k\frac{\partial \mathcal{M}_k}{\partial t} \ ,\end{aligned} \tag{135}$$

we obtain

$$\begin{aligned}\frac{\partial \mathcal{P}_i}{\partial x_i} = \frac{\partial}{\partial t}\Big(P_i E_i - \mathcal{M}_i B_i + \frac{1}{2}(D_k E_k + H_j B_j)\Big) + J_i^{\text{fr.}}E_i - P_i\frac{\partial E_i}{\partial t} + B_k\frac{\partial \mathcal{M}_k}{\partial t} \ , \\ \frac{\partial}{\partial t}\underbrace{\Big(P_i E_i - \mathcal{M}_i B_i + \frac{1}{2}(D_k E_k + H_j B_j)\Big)}_{e^{\text{f.}}} = \frac{\partial \mathcal{P}_i}{\partial x_i} - \underbrace{\Big(J_i^{\text{fr.}}E_i - P_i\frac{\partial E_i}{\partial t} + B_k\frac{\partial \mathcal{M}_k}{\partial t}\Big)}_{\pi} \ ,\end{aligned} \tag{136}$$

D. Maxwell symmetry

The MAXWELL symmetry relations can be seen by using simple relations,

$$\begin{aligned}\tilde{c}_{ji}^{21} = \frac{\partial n_{ji}}{\partial T} = \frac{\partial^2 f}{\partial T\partial F_{ij}} = \frac{\partial^2 f}{\partial F_{ij}\partial T} = -\frac{\partial \eta}{\partial F_{ij}} = -\tilde{c}_{ij}^{12} \ , \\ \tilde{c}_i^{31} = \frac{\partial p_i}{\partial T} = -\frac{\partial^2 f}{\partial T\partial E_i} = -\frac{\partial^2 f}{\partial E_i\partial T} = \frac{\partial \eta}{\partial E_i} = \tilde{c}_i^{13} \ , \\ \tilde{c}_i^{41} = \frac{\partial m_i}{\partial T} = -\frac{\partial^2 f}{\partial T\partial B_i} = -\frac{\partial^2 f}{\partial B_i\partial T} = \frac{\partial \eta}{\partial B_i} = \tilde{c}_i^{14} \ , \\ \tilde{c}^{51} = \frac{\partial p}{\partial T} = -\frac{\partial^2 f}{\partial T\partial \mathrm{v}} = -\frac{\partial^2 f}{\partial \mathrm{v}\partial T} = \frac{\partial \eta}{\partial \mathrm{v}} = \tilde{c}^{15} \ ,\end{aligned} \tag{137}$$

furthermore,

$$\begin{aligned}\tilde{c}_{ikl}^{32} = \frac{\partial p_i}{\partial F_{kl}} = -\frac{\partial^2 f}{\partial F_{kl}\partial E_i} = -\frac{\partial^2 f}{\partial E_i\partial F_{kl}} = -\frac{\partial n_{lk}}{\partial E_i} = -\tilde{c}_{lki}^{23} \ , \\ \tilde{c}_{ikl}^{42} = \frac{\partial m_i}{\partial F_{kl}} = -\frac{\partial^2 f}{\partial F_{kl}\partial B_i} = -\frac{\partial^2 f}{\partial B_i\partial F_{kl}} = -\frac{\partial n_{lk}}{\partial B_i} = -\tilde{c}_{lki}^{24} \ , \\ \tilde{c}_{kl}^{52} = \frac{\partial p}{\partial F_{kl}} = -\frac{\partial^2 f}{\partial F_{kl}\partial \mathrm{v}} = -\frac{\partial^2 f}{\partial \mathrm{v}\partial F_{kl}} = -\frac{\partial n_{lk}}{\partial \mathrm{v}} = -\tilde{c}_{lk}^{25} \ ,\end{aligned} \tag{138}$$

as well as

$$\begin{aligned}\tilde{c}_{ik}^{43} = \frac{\partial m_i}{\partial E_k} = -\frac{\partial^2 f}{\partial E_k\partial B_i} = -\frac{\partial^2 f}{\partial B_i\partial E_k} = \frac{\partial p_k}{\partial B_i} = \tilde{c}_{ki}^{34} \ , \\ \tilde{c}_k^{53} = \frac{\partial p}{\partial E_k} = -\frac{\partial^2 f}{\partial E_k\partial \mathrm{v}} = -\frac{\partial^2 f}{\partial \mathrm{v}\partial E_k} = \frac{\partial p_k}{\partial \mathrm{v}} = \tilde{c}_k^{35} \ ,\end{aligned} \tag{139}$$

and

$$\tilde{c}_k^{54} = \frac{\partial p}{\partial B_k} = -\frac{\partial^2 f}{\partial B_k \partial \mathrm{v}} = -\frac{\partial^2 f}{\partial \mathrm{v} \partial B_k} = \frac{\partial m_k}{\partial \mathrm{v}} = \tilde{c}_k^{45} \ . \tag{140}$$